



HAL
open science

Mechanistic Insights into the Cobalt-Mediated Radical Polymerization (CMRP) of Vinyl Acetate with Cobalt(III) Adducts as Initiators

Antoine Debuigne, Yohan Champouret, Robert Jérôme, Rinaldo Poli,
Christophe Detrembleur

► **To cite this version:**

Antoine Debuigne, Yohan Champouret, Robert Jérôme, Rinaldo Poli, Christophe Detrembleur. Mechanistic Insights into the Cobalt-Mediated Radical Polymerization (CMRP) of Vinyl Acetate with Cobalt(III) Adducts as Initiators. *Chemistry - A European Journal*, 2008, 14 (13), pp.4046-4059. 10.1002/chem.200701867 . hal-03192703

HAL Id: hal-03192703

<https://hal.science/hal-03192703v1>

Submitted on 8 Apr 2021

HAL is a multi-disciplinary open access archive for the deposit and dissemination of scientific research documents, whether they are published or not. The documents may come from teaching and research institutions in France or abroad, or from public or private research centers.

L'archive ouverte pluridisciplinaire **HAL**, est destinée au dépôt et à la diffusion de documents scientifiques de niveau recherche, publiés ou non, émanant des établissements d'enseignement et de recherche français ou étrangers, des laboratoires publics ou privés.

Mechanistic Insights into the Cobalt Mediated Radical Polymerization (CMRP) of Vinyl Acetate with Cobalt(III) Adducts as Initiators

Antoine Debuigne,^[a] Yohan Champouret,^[b] Robert Jérôme,^[a] Rinaldo Poli*^[b] Christophe Detrembleur*^[a]

Abstract: Over the past few years, Cobalt Mediated Radical Polymerization (CMRP) has proved efficiency in controlling the radical polymerization of very reactive monomers, such as vinyl acetate. However, the reason for this success and the intimate mechanism remained basically speculative. In this paper, two mechanisms are shown to co-exist: the Reversible-Termination (RT) of the growing PVAc chains by the Co(acac)₂ complex and a Degenerative chain

Transfer process (DT). The importance of one contribution over the other one strongly depends on the polymerization conditions, including complexation of cobalt by ligands, such as water and pyridine. This very significant progress in the CMRP mechanism relies on the isolation and characterization of the very first cobalt adducts formed in the polymerization medium and their use as CMRP initiators. The structure proposed for these adducts was supported by DFT calculations. Beyond

the control of the VAc polymerization which is the best ever achieved by CMRP, extension to other monomers and substantial progress in macromolecular engineering are now realistic forecasts.

Keywords: controlled radical polymerization · cobalt mediated radical polymerization · alkylcobalt(III) adducts · vinyl acetate

Introduction

The last decades have witnessed a huge research effort devoted to techniques able to control the radical polymerization of a variety of monomers.^[1] The possible macromolecular engineering of the parent polymers under non very demanding conditions was the basic incentive. Three main techniques of controlled radical polymerization (CRP) emerged, i.e., Atom Transfer Radical Polymerization (ATRP),^{[2],[3]} Radical Addition Fragmentation Chain Transfer (RAFT)^{[4]-[8]} and Stable Free Radical Polymerization (SFRP).^{[9]-[12]} Other systems must also be mentioned,^{[13]-[18]} with a special emphasis on the so called "Organometallic Radical Polymerization" (OMRP).^[19] In this context, cobalt complexes^{[20]-[25]}

proved high efficiency in mediating the radical polymerization of vinyl monomers, particularly of "nucleophilic" monomers, whose radical polymerization is not prone to control. For instance, CRP of vinyl acetate was made possible with the assistance of bis(acetylacetonato)cobalt(II), not only in bulk,^[26] but also in suspension^[27] and miniemulsion.^[28] This technique, known as "Cobalt Mediated Radical Polymerization" (CMRP), allows poly(vinyl acetate) (PVAc) and poly(vinyl alcohol) (PVOH, merely upon hydrolysis) to be synthesized with a predetermined molecular weight and to be constitutive components of block copolymers which are very difficult to obtain by other techniques.^{[29]-[32]} Well-defined statistical copolymers^{[33],[34]} could also be prepared and fullerene was successfully grafted by PVAc and PVOH.^[35] Until recently, CMRP was explained by a reversible termination mechanism based on the homolytic cleavage of the terminal Co-C bond.^[26] However, recent studies proposed that a degenerative chain transfer would operate, at least under certain conditions.^{[23]-[25],[36]} This proposal was supported by the persistent control of the vinyl acetate polymerization in the presence of a rather large excess of azo-initiator with respect to the cobalt complex, which is typical of a degenerative chain transfer mechanism.^[36] According to the same study, amino derivatives known for coordination to cobalt complexes, such as pyridine, enhanced the reversible termination of the chains.

There is thus a need for an in-depth mechanistic analysis of the CMRP of VAc, which is a prerequisite for further progress in the field. A basic question to be addressed is the structure of the moiety that caps the propagating chains in the dormant state. In this respect, the synthesis of a model compound able to initiate the

[a] Dr. A. Debuigne, Prof. R. Jérôme, Dr. C. Detrembleur, Center for Education and Research on Macromolecules University of Liège Sart-Tilman, B6a, B-4000 Liège (Belgium) Fax: (+32) 4-366 3497 E-mail: christophe.detrembleur@ulg.ac.be

[b] Dr. Y. Champouret, Prof. R. Poli Laboratoire de Chimie de Coordination, UPR CNRS 8241 liée par convention à l'Université Paul Sabatier et à l'Institut National Polytechnique de Toulouse, 205 Route de Narbonne, 31077 Toulouse, France Fax: (+33) 561553003 E-mail : poli@lcc-toulouse.fr (E-mail)

polymerization and to mediate it is of the utmost importance. A cobalt adduct compound would be a reasonable starting point, similarly to alkoxyamines that proved to be effective initiators and mediators in the SFRP mechanism,^[12] although a free-radical initiator and a nitroxide were originally needed to promote this type of controlled polymerization.^[9] Because synthesis of cobalt adducts by classical organometallic reactions is a problem, an excess of cobalt(II) acetylacetonate was reacted with radicals generated in the CMRP of vinyl acetate. The cobalt species accordingly formed were isolated and characterized with the purpose of collecting a single cobalt adduct. In addition to this synthetic effort, the structure and energy of single model compounds were also investigated by computational tools (DFT studies). Both the experimental observations and the DFT calculations could be unified in quite a consistent mechanism that properly accounts for the effect of the Co ligation on the level of control and kinetics of the VAc polymerization.

Results and Discussion

Synthesis and recovery of cobalt(III) adducts.

As previously reported, radical polymerization of vinyl acetate falls under control when mediated by $\text{Co}(\text{acac})_2$. The ability of this cobalt complex to react with vinyl acetate type radicals and to deactivate them temporarily is the basis of the so-called Cobalt Mediated Radical Polymerization (CMRP). Although the polymerization of vinyl acetate initiated by V-70 at 30°C is controlled in the presence of $\text{Co}(\text{acac})_2$, an induction period of several hours is observed and assumed to be the time needed to generate radicals and convert most of the Co^{II} complex into alkylcobalt(III) derivatives as result of the trapping of the growing PVAc oligomers.^{[26], [37]}

Consistently, the induction period should be suppressed by initiating CMRP of VAc by a model alkyl cobalt^{III} complex. However, alkyl adducts of $\text{Co}(\text{acac})_2$ have not been reported in the scientific literature. Nevertheless, a few alkylcobalt(III) species, mostly model compounds of vitamin B12,^{[38], [39]} are well known and have been extensively studied.^{[40]-[43]} These systems typically feature a planar tetradentate ligand, such as a porphyrin or a Schiff base, which mimics the natural enzyme, an axial alkyl ligand, and an additional axial base trans to the alkyl group which completes the octahedral coordination of Co^{III} . Although a limited number of 5-coordinate $\text{RCo}(\text{L}_4)$ complexes exists,^[44] pentacoordination is not a typical occurrence in Co^{III} coordination chemistry, because of the strong ligand field stabilization energy provided by the octahedral coordination for a low-spin d^6 system.^[45] It is clear that the synthesis of an alkylcobalt(III) complex supported by hard-donor ligands such as acac is expected to be a difficult task due to the sensitivity of the cobalt species to oxygen and temperature (the Co-C bond is quite labile as assessed by the ability to carry out the polymerization close to room temperature).

Different synthetic strategies were envisioned for the preparation of a model $[\text{CH}_3\text{CH}(\text{OOCCH}_3)]\text{Co}(\text{acac})_2$ compound, including one-electron oxidative addition of $\text{CH}_3\text{CH}(\text{OOCCH}_3)\text{Br}$ to $\text{Co}(\text{acac})_2$, generation of $\text{CH}_3\text{COOCH}(\text{CH}_3)^{\cdot}$ radicals from $\text{CH}_3\text{CH}(\text{OOCCH}_3)\text{Br}$ and Sn_2Bu_6 or $\text{Cu}(\text{I})$ complexes in the presence of $\text{Co}(\text{acac})_2$, and addition of $\text{CH}_3\text{CH}(\text{OOCCH}_3)\text{Br}$ to a reduced form of $\text{Co}(\text{acac})_2$, but none of these strategies met with

success. We therefore turned to the same method used to initiate the polymerization, namely radical generation from V-70, followed by addition of these radicals to the VAc monomer and subsequent trapping with $\text{Co}(\text{acac})_2$. The reaction was carried out with an excess of $\text{Co}(\text{acac})_2$ with respect to V-70, in order to collect low molecular weight cobalt adducts (Scheme 1). Actually, the reaction was stopped before the end of the induction period.

After several hours of reaction at 30°C, no significant increase in viscosity was observed, and the monomer conversion, measured gravimetrically, was close to zero, in agreement with a low polymer content, if any. V-70 residues were eliminated by elution of the crude reaction mixture through silica under inert atmosphere. Moreover, two fractions were collected with appropriate eluents (cfr. experimental) and identified as cobalt derivatives by ICP: a minor green compound **1** and a more abundant pink derivative **2**. Formation of two different cobalt species during the induction period was unexpected. Their nature, handling and ability to initiate and control polymerization of vinyl acetate were systematically investigated.

For reasons that will become apparent after examining the probable structure of the product **1**, the above reaction was repeated in the absence of monomer. This procedure led to a final mixture that was worked up in the same way as the mixture leading to the product fractions **1** and **2** above (chromatography on a silica column with $\text{CH}_2\text{Cl}_2/\text{EtOAc}$). A green fraction, the color and elution properties of which are analogous to those of product **1**, was collected, whereas no pink fraction similar to product **2** was obtained in this case.

Characterization of the cobalt(III) adducts

Infrared characterization. Besides the difference in color and solubility properties (elution through silica), compounds **1** and **2** also differ in their IR properties, as shown in Figure 1. Most notable is the presence of a strong and sharp band centred at 2017 cm^{-1} in the spectrum of product **1**, whereas this band is nearly absent in the spectrum of product **2**. Conversely, **2** shows a strong band centred at 1738 cm^{-1} , whereas this band is very small in the spectrum of **1**. The latter absorption is clearly attributable to an ester function of VAc monomer units, suggesting that product **2** might be the expected Co^{III} -capped PVAc oligomer (Scheme 1). On the other hand, product **1** does not seem to contain monomer units (the small residual band at 1738 cm^{-1} in this product could result from the partial migration of **2** under the elution conditions of **1**). It is for this reason that the reaction between $\text{Co}(\text{acac})_2$ and V-70 was repeated in the absence of monomer, leading also to the isolation of ~~the~~ compound **1**, as supported by IR spectroscopy (Figure 1). Note that a carbonyl absorption band at 1738 cm^{-1} is completely absent in this case. Thus, product **1** appears to be a by-product of the CMRP initiating system: V-70 produces primary radicals (R_0) and these are either intercepted by monomer molecules and then terminated by $\text{Co}(\text{acac})_2$, leading to the pink $\text{R}_0\text{-(VOAc)}_n\text{-Co}(\text{acac})_2$ oligomers **2**, or directly react with $\text{Co}(\text{acac})_2$, leading to the green product **1**.

It is reasonable to ask now what the probable structure for this green material **1** is. The absorption at 2017 cm^{-1} is significantly red-shifted from that of a terminal nitrile group (typically in the range $2260\text{-}2240\text{ cm}^{-1}$ and only slightly red-shifted in the presence of conjugation with other organic π systems, e.g. $2240\text{-}2215\text{ cm}^{-1}$ for $\text{C}=\text{C}\equiv\text{N}$ and $\text{Ar-C}\equiv\text{N}$ compounds).^[46] The hypothesis of an

addition of the primary radical to $\text{Co}(\text{acac})_2$ via the carbon does not appear reasonable, because on one hand the CN vibration would not be significantly shifted from that of typical nitrile compounds, and on the other hand the C-Co bond is not expected to be sufficiently strong (see DFT calculations below). An alternative hypothesis is the addition of the primary radical to $\text{Co}(\text{acac})_2$ through the N atom, given that conjugation brings a significant spin density on the N atom, to form a ketiminato ligand, see Scheme 2. A very limited number of ketiminato complexes has been previously described, and these exhibit significantly red-shifted C-N stretching vibrations relative to free nitrile functionalities, e.g. $\text{Cp}^*(\text{PMe}_3)(\text{Ph})\text{Ir}[\text{N}=\text{C}=\text{CPh}_2]$ ($\nu_{\text{CN}} = 2098 \text{ cm}^{-1}$)^[47] and $(\text{dmpe})_2(\text{H})\text{Ru}[\text{N}=\text{C}=\text{CHAr}]$ (Ar = Ph, $\nu_{\text{CN}} = 2120 \text{ cm}^{-1}$; Ar = *p*- $\text{C}_6\text{H}_4\text{CF}_3$, $\nu_{\text{CN}} = 2134 \text{ cm}^{-1}$).^{[48],[49]}

Independent efforts at crystallizing this product in the form of single crystals suitable for an X-ray diffraction study did not meet with success. The compound appears rather unstable, since it is a thermal source of radicals (*vide infra*). During numerous attempts to grow single crystals, mixtures of microcrystalline powder and green crystals were systematically obtained. One of the green crystals, of sufficient quality for an X-ray investigation, turned out to correspond to compound $\text{Co}(\text{acac})_3$.^[50] The white powder exhibited the typical C-N vibration of terminal nitriles ($\nu_{\text{CN}} = 2240 \text{ cm}^{-1}$). Further information on this decomposition process was obtained by NMR spectroscopy (*vide infra*).

DFT Investigation of the green ketiminato by-product. Since we were not able to isolate and fully characterized the ketiminato species shown in Scheme 2, i.e. the likely candidate for the main product obtained from V-70 and $\text{Co}(\text{acac})_2$ as well as the minor product when the same reaction is carried out in the presence of VAc (product **1**), we decided to explore its structure and energy by computational tools. The calculations were carried out using the simpler $(\text{CH}_3)\text{CH}(\text{CN})$ radical in the interest of computational speed.

Qualitatively, one could argue that after formation of the Co-N σ bond, leading to a formally 16-electron $(\text{acac})_2\text{Co}-\text{N}=\text{C}=\text{C}(\text{CH}_3)_2$ complex, the residual lone pair available on the N atom could interact with an empty Co d orbital and yield a stable 5-coordinate complex. This would be an example of the so-called π -stabilized unsaturation.^[51] Under the above assumption, the optimization was started from the most reasonable geometry, namely a trigonal bipyramid with the π -donor ligand in the equatorial plane and oriented in such a way as to form the π bond with the (xy, x^2-y^2) set.^[52] However, to our surprise, the geometry dramatically rearranged and eventually optimized to a square pyramid with the ketiminato ligand located in one of the equatorial positions (Figure 2). Moreover, this structure is endothermic by 20.0 kcal/mol relative to the separated $\text{Co}(\text{acac})_2$ and $\text{C}(\text{CH}_3)_2\text{CN}$ species, but on the other hand the calculated C=N frequency would seem in rather good agreement with the experimental value shown in Figure 1. Indeed, the calculation yields 2101 cm^{-1} , vs. 2305 cm^{-1} for the C-bonded isomer and 2363 cm^{-1} for the $(\text{CH}_3)_2(\text{CN})\text{C}-\text{N}=\text{N}-\text{C}(\text{CN})(\text{CH}_3)_2$ model of V-70. Against expectations, the optimized Co-N-C angle is very much smaller than 180° (133.4°), clearly indicating that no Co-N π interaction is established. Rather, it appears that the N lone pair is still fully localized on the N atoms and ready to establish a σ bond with a second metal atom.

The above result suggested to us that this mononuclear structure would probably gain in stability by forming a Lewis acid-base dimer.

In other words, the N atom of this molecule could donate its lone pair to the Co atom of a second identical molecule, the N atom of which would donate its own lone pair to the Co atom of the first molecule. Indeed, this dinuclear model smoothly optimized to the geometry shown in Figure 2. The system is now exothermic by 9.4 kcal/mol relative to two $\text{Co}(\text{acac})_2$ and two radicals. Furthermore, the calculated C=N frequencies (2117.5 and 2117.8 cm^{-1}) are once again in line with the experimental value.

NMR characterization. Confirming the conclusions drawn in the infrared section, the NMR spectrum of product **1** exhibits far too many resonances, indicating that this product is a complex mixture of different compounds. After the first chromatographic separation, the NMR spectrum (CDCl_3) exhibits resonances at the expected chemical shift for the acac ligand [singlets at δ 5.52 and 2.17] and for the organic groups of R_0 [signals at δ 3.18 (s), 2.59 (d), 2.19 (d), 1.70 (s), 1.27 (s) and 1.21 (s)], but the spectrum changed and simplified after successive chromatographic purifications. The green fraction contains less and less of the resonances of the organic R_0 fragment and only shows the acac ligand resonances, consistent with the quantitative formation of a diamagnetic Co^{III} species. The white powder mentioned in the infrared section was consistent with the simple product of primary radical coupling, $\text{R}_0\text{-R}_0$. These results suggest that the ketiminato species suffers from a variety of complex decomposition processes. The detailed mechanism of its decomposition was not further investigated.

The pink cobalt adduct **2** was analyzed by NMR before and after substitution of the $\text{Co}(\text{acac})_2$ chain-end by TEMPO (product **2'**). TEMPO is indeed a very efficient scavenger of the PVAc radicals generated by cleavage of the PVAc-Co bond.^[53] In this study, the pink cobalt adduct **2**, assumed to be a very low molecular weight PVAc derivative, was reacted with TEMPO. Comparison of the ^1H NMR spectra of **2** and **2'** (Figure 3) confirms the success of the cobalt-TEMPO exchange. The common signals of the two compounds are those of the α end-group (V-70 fragment; signals **e** and **f** between 1.0 and 1.5 ppm, and signal **d** characteristic of $-\text{OCH}_3$ at 3.16 ppm) and those of the VAc units, the penultimate unit excluded (signal **a** corresponding to CHOAc between 4.8 and 5.2 ppm and **b**, corresponding to CH_2 , mixed with other signals between 2.0 and 1.7 ppm). The signals of the PVAc last unit and those of the chain-end attached to such unit differ as expected. For the sake of clarity, those of **2'** are described first. The protons corresponding to the TEMPO can be observed between 1.0 and 1.5 ppm (signals **i** and **j** in Figure 3b). Moreover, the signal **h** corresponding to the CHOAc proton in the final VAc unit, linked to the TEMPO, is downfield-shifted to 6.2 ppm. The latter signal, on the other hand, is absent in the spectrum of **2** and is replaced by a resonance at 2.5 ppm. This spectacular upfield shift is related to the replacement of the electronegative O atom with the electropositive Co atom. The rather large width of resonance **h** in both spectra is due to the expected presence of several contributing species. Firstly, the diade made up of the two last monomer units may be of *r* or *m* type. The *r* diade has a CH_2 group with equivalent H atoms, giving rise to a triplet, while the CH_2 group of the *m* diade has diastereotopic H atoms, giving rise to a doublet of doublets. Radical polymerization is non stereospecific and the two diades are expected in an approximately 1:1 ratio. Secondly, the number of distinct species is further doubled by an additional diastereomeric relationship resulting from the chirality of the cobalt center (*vide infra*).

It is now interesting to observe that the acac ligands of the $\text{Co}(\text{acac})_2$ chain-end are not equivalent, two main **i** resonances for the CH groups being observed at 5.5 and 5.3 ppm. This suggests a *cis* arrangement for the two acac groups in a pseudo-octahedral arrangement, rendering the Co center chiral. The slight splitting observed for the **i** resonances may be attributed to the presence of two different diastereoisomers, differing from the relative configurations of the Co atom and Co-bonded C atom, as mentioned above. The corresponding CH_3 resonances (**j**) overlap with other resonances in the 2.0 to 1.4 ppm region. This bonding picture is fully supported by the DFT calculations, which are described in a later section. The average number of VAc units in the pink cobalt adduct **2** is close to 4, as calculated from the intensity of the proton resonances typical of the VAc units and the chain ends, respectively. In conclusion, compound **2** is very low molecular weight cobalt adduct formed by the rapid trapping of the growing PVAc chains by $\text{Co}(\text{acac})_2$, as suggested in Scheme 1.

Visible –UV characterization. The green cobalt adduct **1** and the pink derivative **2** were also discriminated by UV-visible spectroscopy under inert atmosphere (Figure 4). An absorption maximum was observed at 592 nm for the minor green product **1** and at 516 nm for the pink compound **2**.

Moreover, the absorption profiles changed when these cobalt complexes were handled under different conditions. For example, the pink compound **2** turned green when not purified under inert atmosphere, whereas the coloration of the compound **1** did not change. The sensitivity of the low molecular weight PVAc- $\text{Co}^{\text{III}}(\text{acac})_2$ compound **2** to oxygen was confirmed by the continuous change of the UV-vis spectrum upon exposure to air (Figure 5), together with a color change from pink to green. After 1 hour, the UV-visible curve no longer changed, consistent with the complete conversion of the pink compound **2** into a green product **3**. The latter compound is however different from the minor green product **1**, λ_{max} of compound **3** being 599 nm instead of 592 nm for the green compound **1** (Figure 5).

The UV-visible spectrum of compound **2** does not change upon addition of distilled and degassed water as long as the sample was maintained under an inert atmosphere (Figure 6). In contrast, upon exposure to air, the pink solution **2** turns green, as previously observed. It is thus clear that oxidation is basically responsible for the conversion of the low molecular weight cobalt adduct **2** into the green compound **3** and not coordination of water (air moisture) onto cobalt with formation of a six-coordinated cobalt chain end [PVAc- $\text{Co}(\text{acac})_2(\text{H}_2\text{O})$]. A likely first step of the chemical transformation responsible for the color change is the insertion of a dioxygen molecule into the Co-C bond, to yield an alkylperoxo complex, which then may evolve to other products. A characteristic example of this oxidation process was reported elsewhere, including the X-ray analysis of the alkylperoxo product.^[54]

Polymerization of vinyl acetate initiated by the cobalt(III) adducts.

A key question to address is the ability of the isolated Co adducts **1-3** to initiate the CMRP of VAc and, in case of success, to control it. This study should allow concluding whether the initiation of CMRP takes place according to a degenerative chain transfer

mechanism or by simple cleavage of the cobalt-carbon bond and release of the initiating radical (Scheme 3).

Radical polymerization of vinyl acetate was carried out with compounds **1-3**, respectively. Data are reported in Table 1. When carried out at 30 °C in the presence of the green product **1**, the VAc polymerization is rather fast (10% conversion per hour) although uncontrolled (Table 1, entry 1). Indeed, the molar mass is much higher than expected in case of control and it does not increase with the monomer conversion beyond 20% conversion. Polydispersity of PVAc was also high (~ 2). That the initiator efficiency is low is not surprising in the light of the thermal decomposition process revealed by the above described spectroscopic studies (cfr supra). The complexity of the decomposition reaction, which releases Co^{III} products together with $\text{Co}(\text{acac})_2$, also accounts for the poor control of the process. Nevertheless, the compound **1** is able to form primary radicals under mild conditions but their actual structures are unknown.

In contrast, the vinyl acetate polymerization conducted with the pink cobalt adduct **2** is very slow and controlled (Table 1, entry 2). Indeed, the monomer conversion is only 11% after 7 h, whereas the molar mass increases regularly with the monomer conversion. There is a rather good agreement between experimental and theoretical molar masses and the polydispersity is low along the polymerization (~1.1-1.2). It thus appears that the pink alkyl-cobalt complex **2** is a realistic model for the PVAc- $\text{Co}(\text{acac})_2$ dormant chains. The initiation of the polymerization and the slow consumption of the vinyl acetate in the presence of the purified compound **2** are accounted for by the homolytic cleavage of the C-Co bond and the occurrence of a reversible termination process (pathway a, Scheme 3). However, for the time being, it can not be excluded that a propagating chain, released by the reversible termination mechanism, is involved in a degenerative chain transfer process.

Kinetics of the polymerizations carried out with the cobalt adducts **1** and **2** are compared in Figure 7, which clearly emphasizes a much higher polymerization rate in case of the green cobalt complex **1**.

Polymerization of vinyl acetate initiated by the pink alkyl cobalt complex **2 in the presence of additives.**

Addition of 2,2'-azo-bis-(4-methoxy-2,4-dimethyl valeronitrile) (V-70). It was recently suggested that bulk CMRP of vinyl acetate proceeds by a degenerative chain transfer mechanism (pathway b, Scheme 3) when conducted in the presence of V-70. In order to give credit to this proposal, the VAc polymerization was initiated by the cobalt-adduct **2** in the presence of V-70 (Table 2). Expectedly, the addition of V-70 to the polymerization medium drastically increases the polymerization rate (entries 1 and 2 in Table 2). $M_{n,SEC}$ increases regularly with the monomer conversion, as expected for a controlled process. Nevertheless, the polydispersity also increases with the polymerization progress, which indicates that the control is not ideal. All in all, these observations support that a degenerative chain transfer process contributes to the polymerization in the presence of additional azo-initiator.

Addition of pyridine (Py). Another way to speed up CMRP while maintaining the polymerization control consists in adding electron donating compounds, such as pyridine.^[36] Indeed, it was

reported that bulk CMRP of vinyl acetate initiated by V70 in the presence of $\text{Co}(\text{acac})_2$ was faster and that the induction period disappeared in the presence of pyridine, which is able to coordinate the cobalt complex. It was suggested that this ligand changes the polymerization mechanism from a degenerative chain transfer to a reversible termination process. In this work, a small amount of pyridine was added to the pink cobalt adduct **2**. Expectedly, the polymerization was three times faster when conducted in the presence of a stoichiometric amount of pyridine with respect to the cobalt complex (Table 3 and Figure 8a).

$$\ln[M]_0/[M] = (3k_p/2) (K[P-X]_0/3k_t)^{1/3} t^{2/3} \quad \text{Eq. 1}$$

where k_p and k_t are the rate constants of propagation and termination, respectively.

K is the equilibrium constant between the active and the dormant species.

P-X stands for polymeric dormant species end-capped by the control agent X.

This power law was experimentally observed for polymerizations directly initiated by alkoxyamines, in the absence of conventional radical initiator and free nitroxide.^{[55]-[57]} Similarly to alkoxyamines, the cobalt adduct **2** releases both the initiating radical and the controlling agent ($\text{Co}(\text{acac})_2$). Therefore, it is not surprising to observe a linear 2/3 order dependence of $\ln[M]_0/[M]$ on time for the polymerization carried out with this compound. This observation is an additional evidence that a reversible-termination mechanism operates in the controlled process.

Under these conditions, the polydispersity remains very low (1.10) and the molar mass increases with the monomer conversion. The clear shift of the SEC chromatograms towards shorter elution times when the monomer conversion increases is shown in Figure 9.

Addition of water. Ligation of the $\text{Co}(\text{acac})_2$ by water molecules was also previously suggested. Therefore, the pink cobalt adduct **2** was used in conjunction with water in CMRP of vinyl acetate. The addition of water has a beneficial effect on the polymerization kinetics (compare Table 1 entry 2 and Table 4). Indeed, after 7 h, the monomer conversion increases from 11% to 52% upon addition of water. Figure 10a is another illustration of this drastic kinetic effect.

Moreover, the experimental data reported in Table 4 agree with a controlled polymerization as assessed by the linear relationships between M_n and the monomer conversion (Figure 10 b) and between $\ln[M]_0/[M]$ and $t^{2/3}$ (Figure 10 a). This 2/3-order linear dependence gives credit to a controlled polymerization that proceeds by a reversible termination mechanism in the presence of water.^{[58]-[60]} Moreover, the polydispersity is very low (~ 1.1) and the molar masses are very close to the theoretical values, even at monomer conversions as high as 97%. The excellent level of control imparted to the VAc polymerization by water is nicely illustrated by the shift of the SEC chromatograms towards shorter elution times (Figure 11).

At constant $[\text{H}_2\text{O}]/[\mathbf{2}]$ ratio, the PVAc molar mass is expectedly controlled by the $[\text{VAc}]/[\mathbf{2}]$ ratio as illustrated in Figure 12. It must be noted that PVAc with a molar mass as high as 160000 g/mol and a low polydispersity (1.3) can be prepared in a controlled

manner. The level of control is therefore higher when conducted with the cobalt model compound **2** than with a combination of $\text{Co}(\text{acac})_2$ and V-70.

Impact of water on the course of the CMRP of Vinyl Acetate

The above discussed effect of water on CMRP of VAc was an incentive to revise the discussion of previously reported experiments of CMRP in suspension²⁷ and miniemulsion.²⁸ When carried out by these techniques rather than in bulk, the VAc polymerization was typically much faster while remaining under control. This effect was tentatively explained by the diffusion of the control agent ($\text{Co}(\text{acac})_2$) from the monomer droplets to the aqueous phase, that shifted the equilibrium between active and dormant species towards the active ones. Although this compartmentalization effect cannot be precluded, the ability of water to coordinate the cobalt complex must be taken into account. In this respect, a series of experiments were carried out in order to discriminate these two effects (Figure 13). Right after the induction period, thus as soon as the bulk CMRP of VAc started, the reaction medium was splitted into three parts. The first one was merely maintained at 30°C (●). The dry vinyl acetate of the second part was evaporated and replaced by VAc saturated with water (▲). A large volume of water ($V_{\text{VAc}}/V_{\text{H}_2\text{O}} = 4$) was added to the third fraction that phase separated immediately (■). The significantly faster polymerization when water saturated VAc was substituted for dry VAc has to be accounted for by water coordination to the cobalt complex. This kinetic benefit was however much smaller than the one observed when the experiment was carried out with a large amount of water, that mimics the suspension/miniemulsion conditions. Only an equilibrium displacement in favor of the active species triggered by diffusion of $\text{Co}(\text{acac})_2$ to the aqueous phase, can explain the amplification of the kinetic effect. In the three cases, the VAc polymerization fits a controlled pattern as assessed by the linear dependence of M_n on the monomer conversion and the rather low polydispersity (1.15-1.3) (Figure 14). The much more important discrepancy between theoretical and experimental molar masses observed for biphasic system is more likely the consequence of the compartmentalization effect, as was observed for CMRP in aqueous dispersed media.

Theoretical investigations into the nature of the organometallic chain end in the dormant species.

Attempts carried out in our laboratory to generate, isolate and characterize a model compound of the PVAc- $\text{Co}(\text{acac})_2$ “unimer” have so far been unsuccessful, as detailed in a previous section. For this reason, we have turned to a computational study of the $[\text{CH}_3\text{CH}(\text{OOCCH}_3)]\text{Co}(\text{acac})_2$ unimer model. The question is whether this compound would be sufficiently stable relative to the separated $\text{CH}_3\text{CH}(\text{OOCCH}_3)$ and $\text{Co}(\text{acac})_2$ species and whether it adopts a 5- or a 6-coordinate geometry. When the polymerization is carried out in the presence of additional bases (L), such as water or pyridine, and the polymerization follows a reversible termination mechanism (see section *e les sections ne sont pas numérotées*), one molecule of the base probably adds to the Co center in the dormant species to afford a PVAc- $\text{Co}(\text{acac})_2(\text{L})$ chain end. However, in the absence of added bases, i.e., when the polymerization follows most probably a degenerate transfer mechanism, the structure of the cobalt chain end is less certain. In a recently published study, some of us have reported DFT calculations on a model $\text{CH}_3\text{-Co}(\text{acac})_2$ system.^[36] The system was found to be most stable in a square

pyramidal geometry with the CH₃ in the axial position and with a spin singlet configuration, its enthalpy being -14.55 kcal/mol relative to the separated CH₃ radical and Co(acac)₂ (which adopts a tetrahedral coordination geometry with a spin quartet ground state). That is, BDE(Co-CH₃) = 14.55 kcal/mol. Furthermore, axial coordination of ligands such as pyridine, NH₃ or H₂O further stabilized the system by an additional 9-13 kcal/mol.

In the present study, we wish to address the nature of the dormant species CH₃CH(X)-Co(acac)₂ not only when X = OOCCH₃, model of the PVAc-Co(acac)₂ unimer, but also when X = COOCH₃ and OCH₃, modeling growing poly(methyl acrylate) (PMA) and poly(vinyl methyl ether) (PVME) chains, respectively. The PMA model was selected because it was previously reported that Co(acac)₂ is ineffective in controlling the polymerization of MA.^[26] The other model (PVME) is of interest because previously published DFT calculation showed that its bonds with halides^[58] and dithiocarboxylates^[59] are nearly as strong as those established by the PVAc model. Finally, we have also modeled a R-Co(acac)₂ compound with R = C(CH₃)₂CN as a simpler model (in the interest of computational time) of the primary radical generated from V-70 and in order to assess the possibility that Co(acac)₂ could directly trap this radical.

All R-Co(acac)₂ systems give similar optimized geometries to that previously reported with R = CH₃. These are shown in Figure 15. The BDE(Co-R) energies are reported in Table 5, together with the Co-C bond length. As expected, all systems show weaker Co-C bonds than the previously reported methyl compound. The BDE decreases when X varies in the order OMe > OOCCH₃, but all these values are still positive. On the other hand, the PMA unimer model yields a negative value. This result is in good agreement with the experimental observation that the MA polymerization cannot be controlled in the presence of Co(acac)₂, i.e., this is not a good spin trap for the PMA growing radical chain. The model of the V-70 primary radical also gives a negative BDE. This is expected from the highly stabilized nature of the resulting radical (tertiary carbon, conjugation with the CN group) and illustrates the principle that the primary radicals are not likely to be trapped by Co(acac)₂ with formation of Co-C bonds. Rather, they are trapped by formation of Co-N bonds (*cf. supra*). Note that cobalt porphyrin complexes are capable of controlling the polymerization of MA,^[20] suggesting that the Co-R bonds are stronger in the presence of a porphyrin ancillary ligand. A theoretical investigation of ancillary ligand effects on the Co-R BDE, however, is beyond the scope of the present work. From Table 5, it can be seen that the optimized Co-C bond length does not correlate in a simple way with the Co-C homolytic bond strength. For instance, whereas the bond is expectedly longer for the weaker bond [with C(CH₃)₂(CN)] and shorter for the stronger bond (with CH₃), the system with CH(CH₃)OCH₃ also shows a rather long bond. Although one may invoke the different contribution of steric, polar and resonance effects in determining strength on one side and length on the other, the way in which these effects operate is not obvious to deduce from these limited data.

We have also investigated the possibility that the carbonyl group of the acetate substituent fills the 6th coordination position at Co^{III}, yielding a more stable octahedral complex, [(κ²:C,O)-CH₃CH(OOCCH₃)]Co(acac)₂, since the NMR study suggests that this may be the structure adopted by the chain-end in the dormant state. Indeed, formation of the 5-membered ring stabilizes the X = OOCCH₃ system by over 6 additional kcal/mol. The optimized

geometry is also shown in Figure 15. Note that the Co(acac)₂ geometry has rearranged in order to make two mutually cis coordination sites available for the alkyl group chelation. An analogous stabilization is not possible for the X = COOMe system, because this would lead to a strained 4-membered ring. Indeed, we find that the local minimum for such [(κ²:C,O)-CH₃CH(COOCH₃)]-Co(acac)₂ model system has a higher energy than the (κ¹:C) minimum shown in Figure 15. To conclude ~~this section~~, the DFT calculations support the suggestion that the PVAc-Co(acac)₂ dormant chain in the vinyl acetate CMRP (occurring via degenerative transfer in the absence of added Lewis bases) contains a 6-coordinate Co^{III} center where the growing PVAc chain adopts a chelating coordination mode, as represented in Figures 3a and 15.

Conclusion

This paper reports for the first time the isolation of low molecular weight cobalt adducts formed at the very early stage of the CMRP of vinyl acetate. Combination of spectroscopic studies, DFT calculations and polymerizations tests allowed to understand how the Co(acac)₂/V-70 pair initiates and controls this radical polymerization (Scheme 4).

Briefly, two cobalt adducts are formed in the polymerization medium during the induction period, i.e., a minor green compound identified as a ketiminatocobalt dimer complex prone to decomposition and a major pink derivative which is an oligomer end-capped by Co(acac)₂ containing an average number of four VAc units (Scheme 4). According to DFT calculations, the carbonyl group of the terminal VAc unit of the pink derivative is coordinated to cobalt, which stabilizes the complex. In contrast to the green compound, the pink PVAc-Co(acac)₂ oligomer is a very efficient CMRP initiator and the VAc polymerization is then very slow. However, the addition of V-70 to the polymerization medium increases the polymerization rate while maintaining a reasonable control, which supports the idea that the system is then dominated by a degenerative chain transfer mechanism. Moreover, a drastic increase in the polymerization rate can also be triggered by ligating Co with pyridine or water. Parallel to this favorable kinetic effect, the best control ever achieved of the VAc polymerization is observed. In this case, the CMRP process proceeds through a reversible-termination mechanism. The role of the Lewis base is to saturate the free coordination site left available by Co^{III}-C bond rupture as previously established.^[36] The Co^{II} species is energetically stabilized and the radical formation equilibrium is shifted to the right.

Finally, it is clear now that water plays a key role whenever CMRP is carried out in aqueous dispersed media. The in-depth analysis of the CMRP mechanism reported in this work is the best lever possible for CMRP to contribute effectively to the macromolecular engineering of usually reluctant polymers.

Experimental Section

Materials. Vinyl acetate (VAc) (>99%, Acros) was dried over calcium hydride, degassed by several freeze-thawing cycles before being distilled under reduced pressure and stored under argon. Ethyl acetate (EtOAc) and dichloromethane (CH₂Cl₂) were dried over molecular sieves and degassed by bubbling argon for 30 min. 2,2'-Azo-bis-(4-methoxy-2,4-dimethyl valeronitrile) (V-70) (Wakko), cobalt(II) acetylacetonate

(Co(acac)₂) (>98%, Acros), 2,2,6,6-tetramethylpiperidine 1-oxy (TEMPO) (98%, Aldrich), and pyridine (Aldrich, > 99%) were used as received.

Characterization.

¹H NMR spectra were recorded with a Bruker AM 250 Spectrometer (250MHz) in deuterated chloroform. Infra-red spectra were recorded with a Perkin Elmer FT-IR in the 4000 to 600 cm⁻¹ range. Low molecular weight cobalt adducts were dissolved in CH₂Cl₂ and solvent-cast on a NaCl disk before IR analysis. Inductively Coupled Plasma Mass Spectrometry (ICPMS) was carried out with a Spectrometer Elan DRC-e Perkin Elmer SCIEX. Samples were prepared as follows : 1 ml of the cobalt adduct stock solution in CH₂Cl₂ was let to evaporate, the residue was treated by 1 ml HNO₃ (65%) at 60°C for 2h, and the reaction mixture was diluted with 250ml of twice distilled water. UV-visible spectra were recorded with a Hewlett Packard 8453 Spectrophotometer, using the pure solvent as a reference. Size exclusion chromatography (SEC) of poly(vinyl acetate) was carried out in THF (flow rate : 1mL min⁻¹) at 40 °C with a Waters 600 liquid chromatograph equipped with a 410 refractive index detector and styragel HR columns (four columns HP PL gel 5μm 10⁵Å, 10⁴Å, 10³Å, 10²Å).

Synthesis and recovery of cobalt(III) adducts 1 and 2. Co(acac)₂ (10 g, 39 mmol) and V-70 (9.25 g, 31 mmol) were added into a round bottom flask capped by a three-way stopcock and purged by three vacuum-argon cycles. After addition of degassed vinyl acetate (75 ml, 813 mmol), the reaction mixture was heated at 30 °C under stirring for 70 h. The medium remained pink all along the polymerization, and no increase in viscosity was observed. The residual monomer was then evaporated under reduced pressure at room temperature, and the residue was placed under argon before being dissolved (or at least dispersed) in dry and degassed CH₂Cl₂. The solution was then transferred with a canula at the top of a silica gel column prepared as follows. A column, equipped with a three-way stopcock at the top and a 1 l flask at the bottom, was filled with silica with the assistance of CH₂Cl₂ eluant. The column was placed under argon and eluted with 1 l of dry and degassed CH₂Cl₂ before the crude reaction product was deposited for chromatographic separation, while avoiding any exposure to air. After the elimination of V-70 residue with CH₂Cl₂, a green fraction was collected with a CH₂Cl₂/EtOAc mixture (85/15) as eluant. Finally, a pink fraction was eluted with EtOAc. The two fractions were evaporated to dryness, and the collected green **1** and pink **2** cobalt adducts were stored at -20°C under argon before stock solutions were prepared for analysis. The green cobalt adduct **1** and the pink cobalt adduct **2** were dissolved, respectively, in 4 ml and 10 ml of degassed CH₂Cl₂. The cobalt concentration of these solutions was measured by ICP ([Co(**1**)] = 1.40 10⁻¹ M and [Co(**2**)] = 2.27 10⁻¹ M).

Synthesis of the cobalt complex 1 in absence of VAc. Co(acac)₂ (5.00 g, 20.0 mmol) and V-70 (4.60 g, 15.5 mmol) were added into a round bottom flask capped by a three-way stopcock and purged by three vacuum-argon cycles. After addition of degassed and distilled anisole (50.0 ml, 46.7g, 542 mmol), the reaction mixture was heated at 30°C under stirring for 120 h. The solvent was then evaporated under reduced pressure at 30°C and the crude mixture was eluted through silica gel under inert atmosphere as aforementioned. After elimination of V-70 by elution with degassed CH₂Cl₂, a green compound **1** was recovered with a CH₂Cl₂/EtOAc mixture (85/15) as eluant. No pink compound was however collected by elution with EtOAc. This fraction was evaporated to dryness under reduced pressure and analyzed by IR, NMR and UV.

Reaction of the pink cobalt adduct 2 with TEMPO. Under an inert atmosphere, the pink cobalt adduct **2** (0.33 mmol, estimated by ICP) and a 10-fold molar excess of 2,2,6,6-tetramethylpiperidine 1-oxy (TEMPO) (500 mg, 3.2 mmol) were dissolved in absolute ethanol (20 ml), previously degassed by bubbling of argon for 20 min. The solution was then heated at 50°C for 24 h. Upon cooling to room temperature, the released Co(acac)₂ crystallized and was eliminated by filtration. After solvent evaporation under reduced pressure at 72°C, the reaction mixture was analyzed by ¹H NMR in CDCl₃.

VAc polymerization initiated by the cobalt(III) adducts. In a round bottom flask capped by a three-way stopcock and purged by three vacuum-argon cycles, 1 ml of the pink cobalt adduct **2** solution ([Co] = 2.27 10⁻¹ M, 0.227 mmol) was added and evaporated to dryness under reduced pressure. Again under an argon atmosphere, degassed vinyl acetate (5 ml, 4.67 g, 54.2 mmol) was added and the reaction mixture was heated at 30 °C under stirring. Samples were regularly picked out and both the monomer conversion (gravimetry) and the molecular weight of PVAc (SEC) were determined. Prior analyses, a tiny amount of TEMPO was added in each sample in order to prevent post coupling reactions. The same experiment was repeated with the green compound **1** and with the green low molecular weight cobalt adduct **3** merely collected after exposure of the pink compound **2** to air (see Results and Discussion section).

VAc polymerization initiated by the cobalt(III) adduct 2 in the presence of additives. In a round bottom flask capped by a three-way stopcock and purged by three vacuum-argon cycles, 1 ml of the pink cobalt adduct **2** solution ([Co] = 2.27 10⁻¹ M, 0.227 mmol) was added and evaporated to dryness under reduced pressure. Again under an

argon atmosphere, degassed vinyl acetate (5 ml, 4.67 g, 54.2 mmol) was added, followed by V-70 (0.02 mmol), pyridine (0.229 mmol) or water (2.20 mmol) and heating at 30 °C under stirring. Samples were regularly picked out from the polymerization medium to monitor both the monomer conversion (gravimetry) and the molecular weight of PVAc (SEC).

General recipe for the cobalt mediated radical polymerization of vinyl acetate added with water at the end of the induction period. Co(acac)₂ (81 mg, 0.3 mmol) and V-70 (270 mg, 0.9 mmol) were added into a round bottom flask capped by a three-way stopcock and purged by three vacuum-argon cycles. After addition of degassed vinyl acetate (15 ml, 14.04 g, 162 mmol), the reaction mixture was heated at 30 °C under stirring. After the induction period of 21h, the monomer conversion was estimated at 4% (gravimetry) and the pink polymerization medium was divided into three parts of 4 ml each (0.08 mmol of Co(acac)₂, 43.2 mmol of VAc). The first part was evaporated to dryness under vacuum at room temperature and then added with 4 ml of VAc previously saturated with water. The second part was merely added with 1 ml of twice distilled and degassed water (V_{VAc}/V_{H₂O} = 4). Polymerization was kept running in the last part, that was thus a reference. In all the cases, polymerization was conducted at 30 °C under an inert atmosphere. Samples were regularly withdrawn and both the monomer conversion (gravimetry) and the molecular weight of PVAc (SEC) were determined.

Computational details. All geometry optimizations were performed using the B3LYP three-parameter hybrid density functional method of Becke,^[60] as implemented in the Gaussian03 suite of programs.^[61] The basis functions consisted of the standard 6-31G** for all light atoms (H, C, N, O), plus the LANL2DZ function, which included the Hay and Wadt effective core potentials (ECP),^[62] for Co. The latter basis set was however augmented with an *f* polarization function ($\alpha = 0.8$) in order to obtain a balanced basis set and to improve the angular flexibility of the metal functions. All geometry optimizations were carried out without any symmetry constraint and all final geometries were characterized as local minima of the potential energy surface (PES) by verifying that all second derivatives of the energy were positive. The unrestricted formulation was used for open-shell molecules. The mean value of the spin of the first-order electron wave function, which is not an exact eigenstate of S² for unrestricted calculations on open-shell systems, was considered to identify unambiguously the spin state. The value of <S²> at convergence was very close to the expected value of 0.75 for the radical species, indicating minor spin contamination. All energies were corrected for zero point vibrational energy and for thermal energy to obtain the bond dissociation enthalpies at 298 K. The standard approximations for estimating these corrections were used (ideal gas, rigid rotor and harmonic oscillator) as implemented into Gaussian03.

Acknowledgements

The authors from Liège are indebted to the "Belgian Science Policy" for financial support in the frame of the "Interuniversity Attraction Poles Programme (PAI VI/27) – Functional Supramolecular Systems", and to the Fonds National de la Recherche Scientifique (F.N.R.S., Belgium). The authors thank Wako for kindly providing them with V70. The authors are much indebted to M. Dejenefte and G. Cartigny for skillful assistance. A. D. and C. D. are "Chargé de Recherche" and "Chercheur Qualifié" by the F.N.R.S., respectively. The authors from Toulouse wish to thank the "Agence National de la Recherche" (Contract No. NT05-2_42140) and the "Centre Interuniversitaire de Calcul de Toulouse" (Project CALMIP) for granting free computational time.

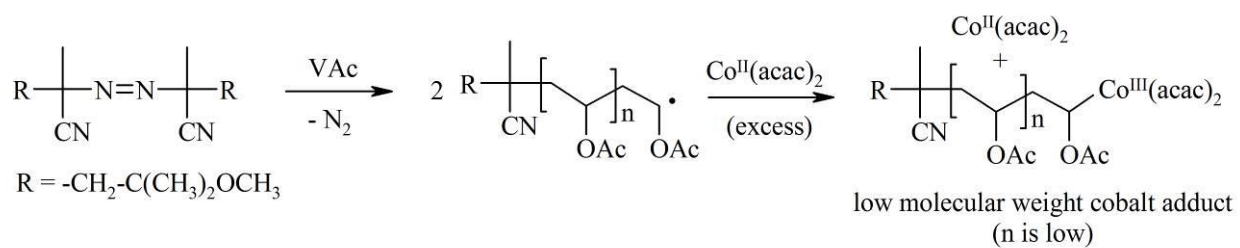
- [1] W. A. Braunecker and K. Matyjaszewski, *Prog. Polym. Sci.* **2007**, *32*, 93-146.
- [2] K. Matyjaszewski and J. Xia, *Chem. Rev.* **2001**, *101*, 2921-2990.
- [3] M. Kamigaito, T. Ando and M. Sawamoto, *Chem. Rev.* **2001**, *101*, 3689-3745.
- [4] G. Moad, J. Chiefari, Y. K. Chong, J. Krstina, R. T. A. Mayadunne, A. Postma, E. Rizzardo and S. H. Thang, *Polym. Int.* **2000**, *49*, 993-1001.
- [5] G. Moad, E. Rizzardo and S. H. Thang, *Aust. J. Chem.* **2005**, *58*, 379-410.
- [6] J. T. Lai, D. Filla and R. Shea, *Macromolecules* **2002**, *35*, 6754-6756.
- [7] J. Chiefari, Y. K. Chong, F. Ercole, J. Krstina, J. Jeffery, T. P. T. Le, R. T. A. Mayadunne, G. F. Meijs, C. L. Moad, G. Moad, E. Rizzardo and S. H. Thang, *Macromolecules* **1998**, *31*, 5559-5562.
- [8] S. Perrier, P. Takolpuckdee and C. A. Mars, *Macromolecules* **2005**, *38*, 2033-2036.
- [9] M. K. Georges, R. P. N. Veregin, P. M. Kazmaier and G. K. Hamer, *Macromolecules* **1993**, *26*, 2987-2988.
- [10] C. J. Hawker, A. W. Bosman and E. Harth, *Chem. Rev.* **2001**, *101*, 3661-3688.
- [11] S. Grimaldi, J.-P. Finet, F. Le Moigne, A. Zeghdaoui, P. Tordo, D. Benoit, M. Fontanille and Y. Gnanou, *Macromolecules* **2000**, *33*, 1141-1147.

- [12] D. Benoit, V. Chaplinski, R. Braslau and C. J. Hawker, *J. Am. Chem. Soc.* **1999**, *121*, 3904-3920.
- [13] Y. Kwak, A. Goto, T. Fukuda, Y. Kobayashi and S. Yamago, *Macromolecules* **2006**, *39*, 4671-4679.
- [14] S. Yamago, B. Ray, K. Iida, J. Yoshida, T. Tada, K. Yoshizawa, Y. Kwak, A. Goto and T. Fukuda, *J. Am. Chem. Soc.* **2004**, *126*, 13908-13909.
- [15] S. Yamago, E. Kayahara, M. Kotani, B. Ray, Y. Kwak, A. Goto and T. Fukuda, *Angew. Chem., Int. Ed.* **2007**, *46*, 1304-1306.
- [16] T. C. Chung, W. Janvikul and H. L. Lu, *J. Am. Chem. Soc.* **1996**, *118*, 705-706.
- [17] T. C. Chung, H. Hong, Z. C. Zhang and Z. M. Wang, *ACS Symp. Ser.* **2006**, *944*, 387-403.
- [18] J.-R. Caille, A. Debuigne and R. Jerome, *Macromolecules* **2005**, *38*, 27-32.
- [19] R. Poli, *Angew. Chem., Int. Ed.* **2006**, *45*, 5058-5070.
- [20] B. B. Wayland, G. Posznmik, S. L. Mukerjee and M. Fryd, *J. Am. Chem. Soc.* **1994**, *116*, 7943-7944.
- [21] B. B. Wayland, L. Basicckes, S. Mukerjee, M. Wei and M. Fryd, *Macromolecules* **1997**, *30*, 8109-8112.
- [22] B. B. Wayland, S. Mukerjee, G. Posznmik, D. C. Woska, L. Basicckes, A. A. Gridnev, M. Fryd and S. D. Ittel, *ACS Symp. Ser.* **1998**, *685*, 305-315.
- [23] B. B. Wayland, X. Fu, Z. Lu and M. Fryd, *Polym. Prep.* **2005**, *46*, 370-371.
- [24] B. B. Wayland, C.-H. Peng, X. Fu, Z. Lu and M. Fryd, *Macromolecules* **2006**, *39*, 8219-8222.
- [25] C.-H. Peng, M. Fryd and B. B. Wayland, *Macromolecules* **2007**, *40*, 6814-6819.
- [26] A. Debuigne, J.-R. Caille and R. Jerome, *Angew. Chem., Int. Ed.* **2005**, *44*, 1101-1104.
- [27] A. Debuigne, J.-R. Caille, C. Detrembleur and R. Jerome, *Angew. Chem., Int. Ed.* **2005**, *44*, 3439-3442.
- [28] C. Detrembleur, A. Debuigne, R. Bryaskova, B. Charleux and R. Jerome, *Macromol. Rapid Commun.* **2006**, *27*, 37-41.
- [29] A. Debuigne, J.-R. Caille, N. Willet and R. Jerome, *Macromolecules* **2005**, *38*, 9488-9496.
- [30] R. Bryaskova, N. Willet, A. Debuigne, R. Jerome and C. Detrembleur, *J. Polym. Sci., Part A: Polym. Chem.* **2006**, *45*, 81-89.
- [31] R. Bryaskova, N. Willet, P. Degee, P. Dubois, R. Jerome and C. Detrembleur, *J. Polym. Sci., Part A: Polym. Chem.* **2007**, *45*, 2532-2542.
- [32] A. Debuigne, N. Willet, R. Jerome and C. Detrembleur, *Macromolecules* **2007**, *40*, 7111-7118.
- [33] H. Kaneyoshi and K. Matyjaszewski, *Macromolecules* **2005**, *38*, 8163-8169.
- [34] H. Kaneyoshi and K. Matyjaszewski, *Macromolecules* **2006**, *39*, 2757-2763.
- [35] C. Detrembleur, O. Stoilova, R. Bryaskova, A. Debuigne, A. Mouithys-Mickalad and R. Jerome, *Macromol. Rapid Commun.* **2006**, *27*, 498-504.
- [36] S. Maria, H. Kaneyoshi, K. Matyjaszewski and R. Poli, *Chem. Eur. J.* **2007**, *13*, 2480-2492.
- [37] A. Debuigne, C. Detrembleur, R. Bryaskova, J.-R. Caille and R. Jerome, *ACS Symp. Ser.* **2006**, *944*, 372-386.
- [38] R. H. Abeles and D. Dolphin, *Acc. Chem. Res.* **1976**, *9*, 114-120.
- [39] K. P. Jensen and U. Ryde, *J. Am. Chem. Soc.* **2005**, *127*, 9117-9128.
- [40] G. N. Schrauzer and R. J. Windgassen, *J. Am. Chem. Soc.* **1966**, *88*, 3738-3743.
- [41] G. N. Schrauzer, *Angew. Chem., Int. Ed.* **1976**, *15*, 417-426.
- [42] L. Randaccio, *Comments Inorg. Chem.* **1999**, *21*, 327-376.
- [43] K. H. Reddy, *Resonance* **1999**, *4*, 67-77.
- [44] R. D. W. Kemmitt and D. R. Russell, in "Comprehensive Organometallic Chemistry"; Eds.: G. Wilkinson, F. G. A. Stone, E. W. Abel; Pergamon Press, Oxford **1982**, *5*, 1-276.
- [45] J. E. Huheey, E. A. Keiter and R. L. Keiter, in "Inorganic Chemistry. Principles of Structure and Reactivity", 4th Ed.; Harper & Row, New York **1993**.
- [46] E. C. Pretsch, T.; Seibl, J.; Simon, W., in "Spectral Data for Structure Determination of Organic Compounds". 2nd Ed.; Springer-Verlag; Berlin **1983**.
- [47] D. M. Tellers, J. C. M. Ritter and R. G. Bergman, *Inorg. Chem.* **1999**, *38*, 4810-4818.
- [48] J. R. Fulton, M. W. Bouwkamp and R. G. Bergman, *J. Am. Chem. Soc.* **2000**, *122*, 8799-8800.
- [49] J. R. Fulton, S. Sklenak, M. W. Bouwkamp and R. G. Bergman, *J. Am. Chem. Soc.* **2002**, *124*, 4722-4737.
- [50] G. J. Kruger and E. C. Reynhardt, *Acta Crystallogr., Sect. B: Struct. Crystallogr. Cryst. Chem.* **1974**, *30*, 822-824.
- [51] K. G. Caulton, *New J. Chem.* **1994**, *18*, 25-41.
- [52] A. R. Rossi and R. Hoffmann, *Inorg. Chem.* **1975**, *14*, 365-374.
- [53] A. Debuigne, J.-R. Caille and R. Jerome, *Macromolecules* **2005**, *38*, 5452-5458.
- [54] W. Mikolajski, G. Baum, W. Massa and R. W. Hoffmann, *J. Organomet. Chem.* **1989**, *376*, 397-405.
- [55] H. Fischer, *Macromolecules* **1997**, *30*, 5666-5672.
- [56] T. Fukuda, A. Goto and K. Ohno, *Macromol. Rapid Commun.* **2000**, *21*, 151-165.
- [57] A. Goto, T. Fukuda, *Prog. Polym. Sci.* **2004**, *29*, 329-385.
- [58] M. B. Gillies, K. Matyjaszewski, P.-O. Norrby, T. Pintauer, R. Poli and P. Richard, *Macromolecules* **2003**, *36*, 8551-8559.
- [59] K. Matyjaszewski and R. Poli, *Macromolecules* **2005**, *38*, 8093-8100.
- [60] A. D. Becke, *J. Chem. Phys.* **1993**, *98*, 5648-5652.
- [61] G. W. T. M. J. Frisch, H. B. Schlegel, G. E. Scuseria, M. A. Robb, J. R. Cheeseman, J. Montgomery, J. A., T. Vreven, K. N. Kudin, J. C. Burant, J. M. Millam, S. S. Iyengar, J. Tomasi, V. Barone, B. Mennucci, M. Cossi, G. Scalmani, N. Rega, G. A. Petersson, H. Nakatsuji, M. Hada, M. Ehara, K. Toyota, R. Fukuda, J. Hasegawa, M. Ishida, T. Nakajima, Y. Honda, O. Kitao, H. Nakai, M. Klene, X. Li, J. E. Knox, H. P. Hratchian, J. B. Cross, C. Adamo, J. Jaramillo, R. Gomperts, R. E. Stratmann, O. Yazyev, A. J. Austin, R. Cammi, C. Pomelli, J. W. Ochterski, P. Y. Ayala, K. Morokuma, G. A. Voth, P. Salvador, J. J. Dannenberg, V. G. Zakrzewski, S. Dapprich, A. D. Daniels, M. C. Strain, O. Farkas, D. K. Malick, A. D. Rabuck, K. Raghavachari, J. B. Foresman, J. V. Ortiz, Q. Cui, A. G. Baboul, S. Clifford, J. Cioslowski, B. B. Stefanov, G. Liu, A. Liashenko, P. Piskorz, I. Komaromi, R. L. Martin, D. J. Fox, T. Keith, M. A. Al-Laham, C. Y. Peng, A. Nanayakkara, M. Challacombe, P. M. W. Gill, B. Johnson, W. Chen, M. W. Wong, C. Gonzalez, J. A. Pople, **2004**.
- [62] P. J. Hay and W. R. Wadt, *J. Chem. Phys.* **1985**, *82*, 270-283.

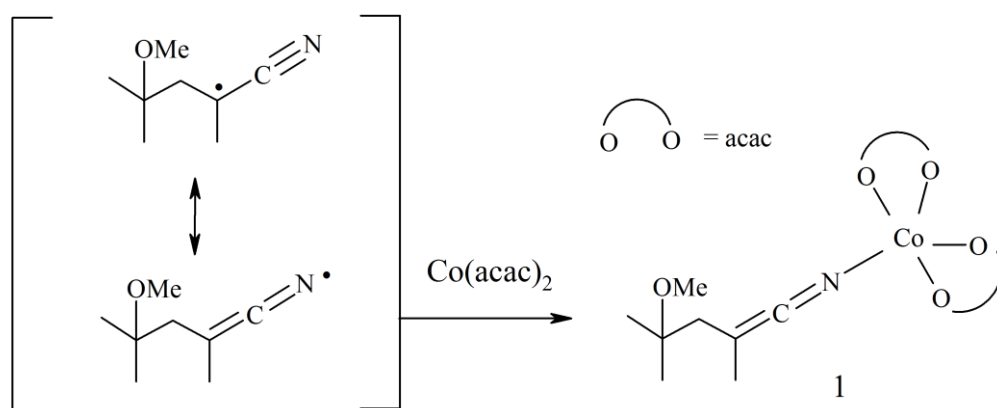
Received: ((will be filled in by the editorial staff))

Revised: ((will be filled in by the editorial staff))

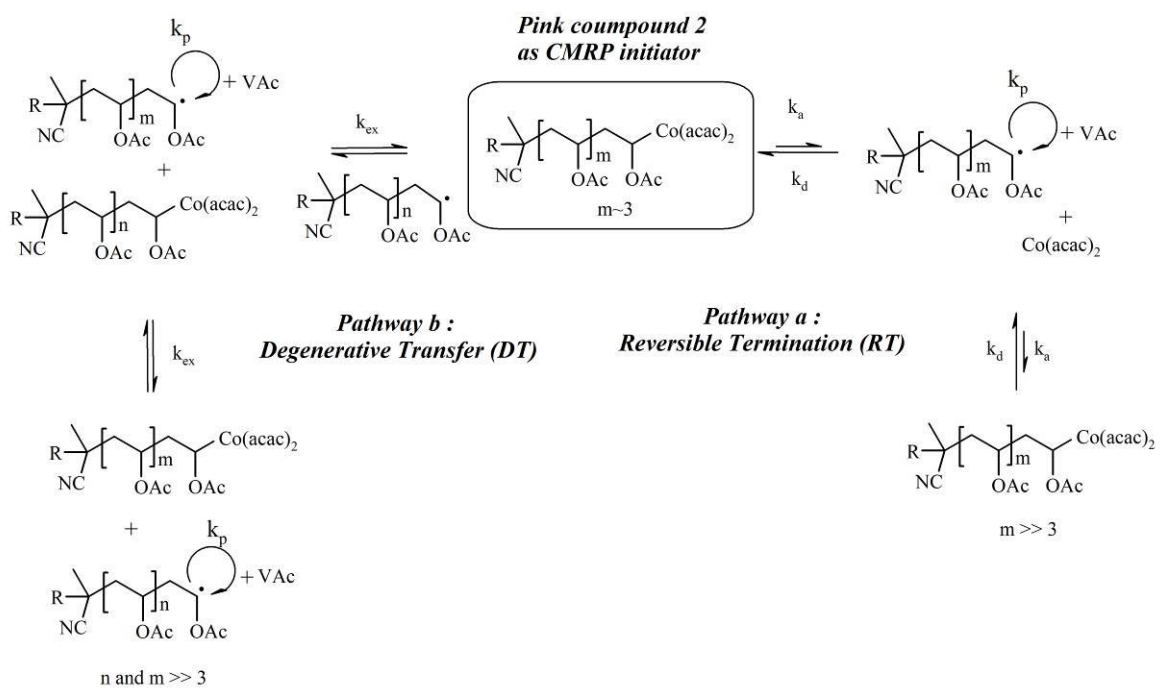
Published online: ((will be filled in by the editorial staff))



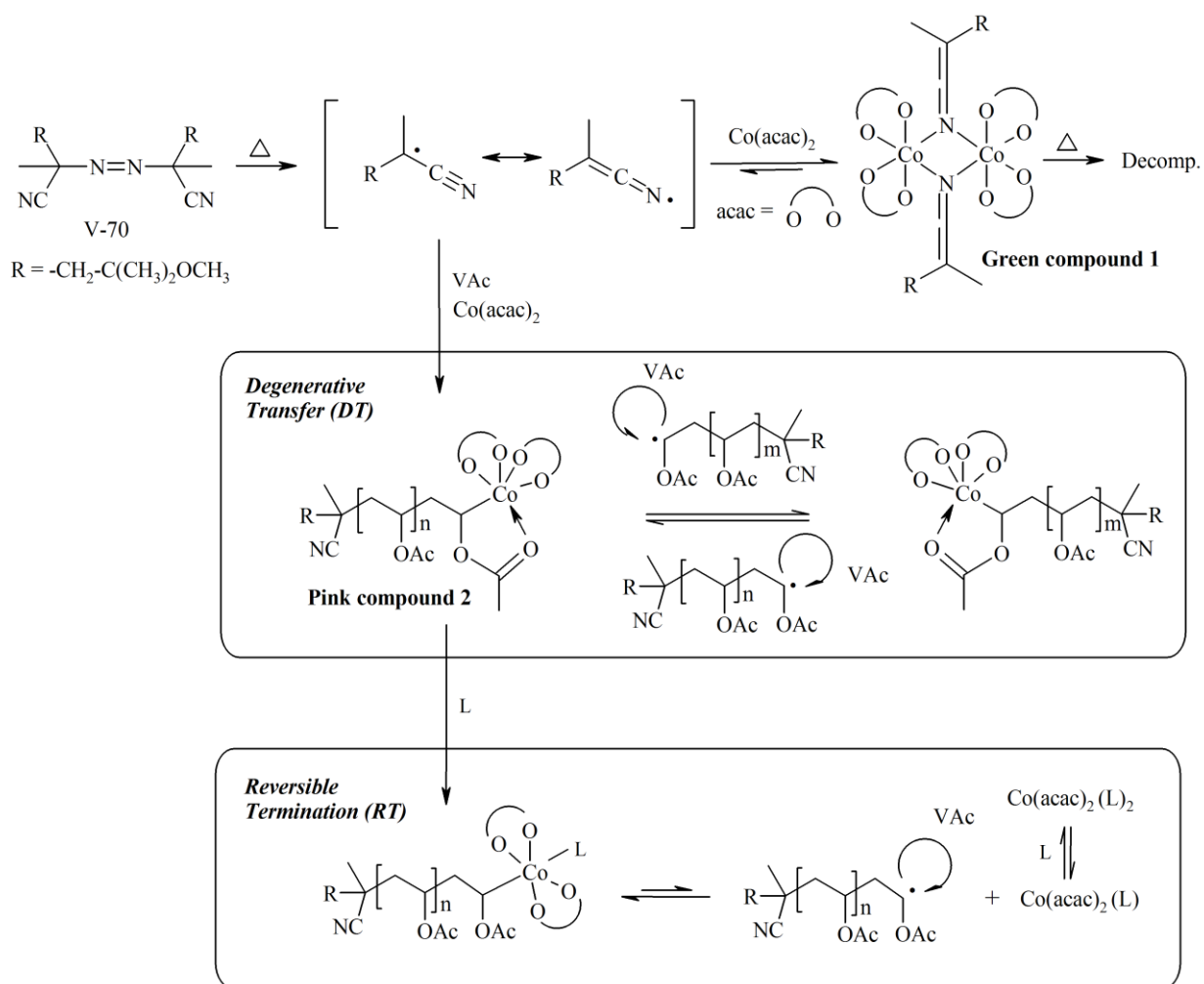
Scheme 1. General strategy for the formation of low molecular weight cobalt adducts by CMRP (reaction time < induction period time).



Scheme 2. Hypothesis for the generation and nature of the green products **1**.



Scheme 3. Possible mechanisms of reversible termination and degenerative chain transfer in CMRP of VAc initiated by a model cobalt adduct.



Scheme 4. Summary of the CMRP initiating system.

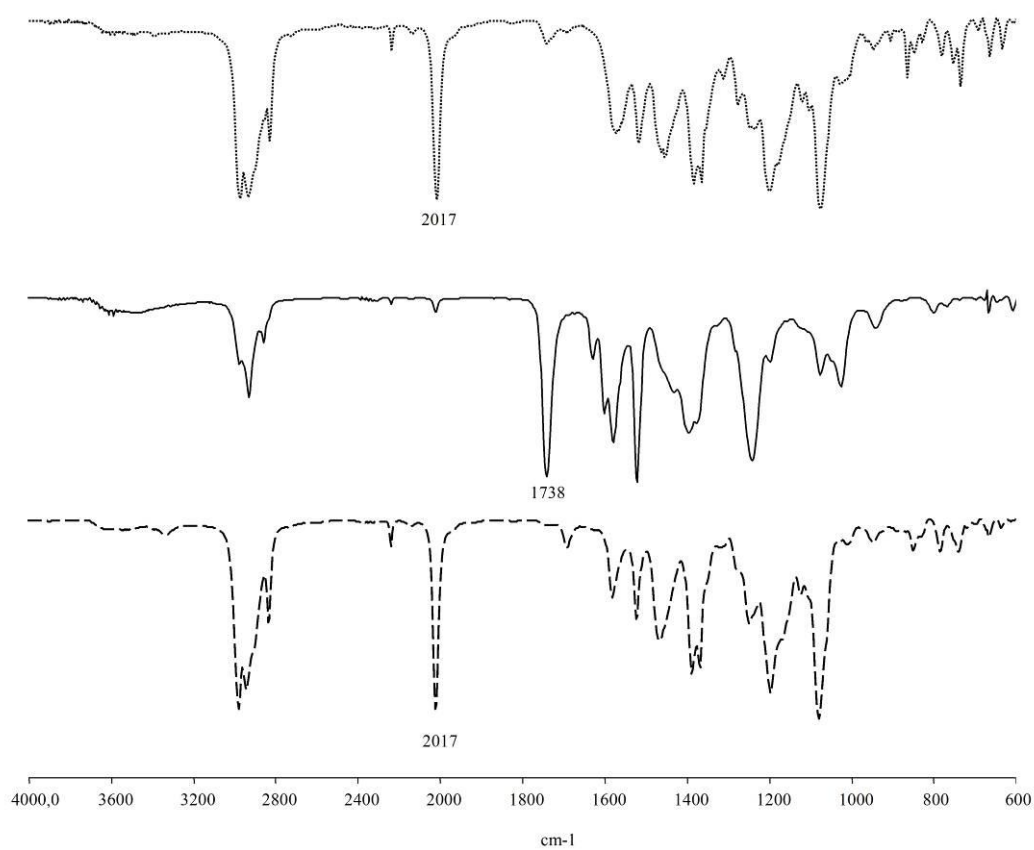


Figure 1. Infra-red spectra of green cobalt adduct **1** (····) and pink cobalt adduct **2** (—) collected when reaction between V-70 and Co(acac)₂ was carried out in the presence of VAc. IR spectrum of green cobalt adduct **1** formed by reaction of V-70 and Co(acac)₂ without VAc (---). The cobalt adducts were dissolved in CH₂Cl₂ and solvent-cast on a NaCl disk before IR analysis.

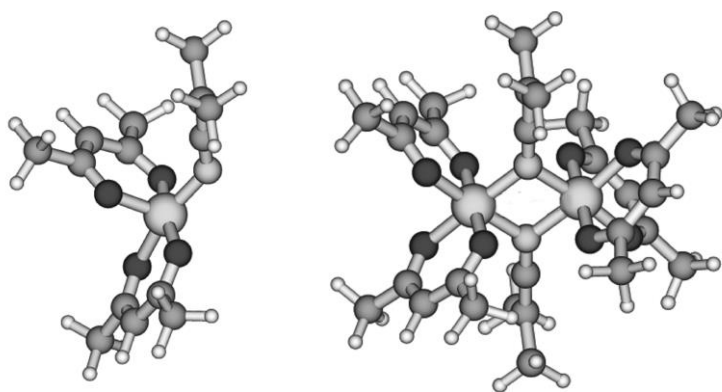


Figure 2. DFT optimized geometries of mononuclear (left) and dinuclear (right) $(acac)_2Co-N=C=C(CH_3)_2$

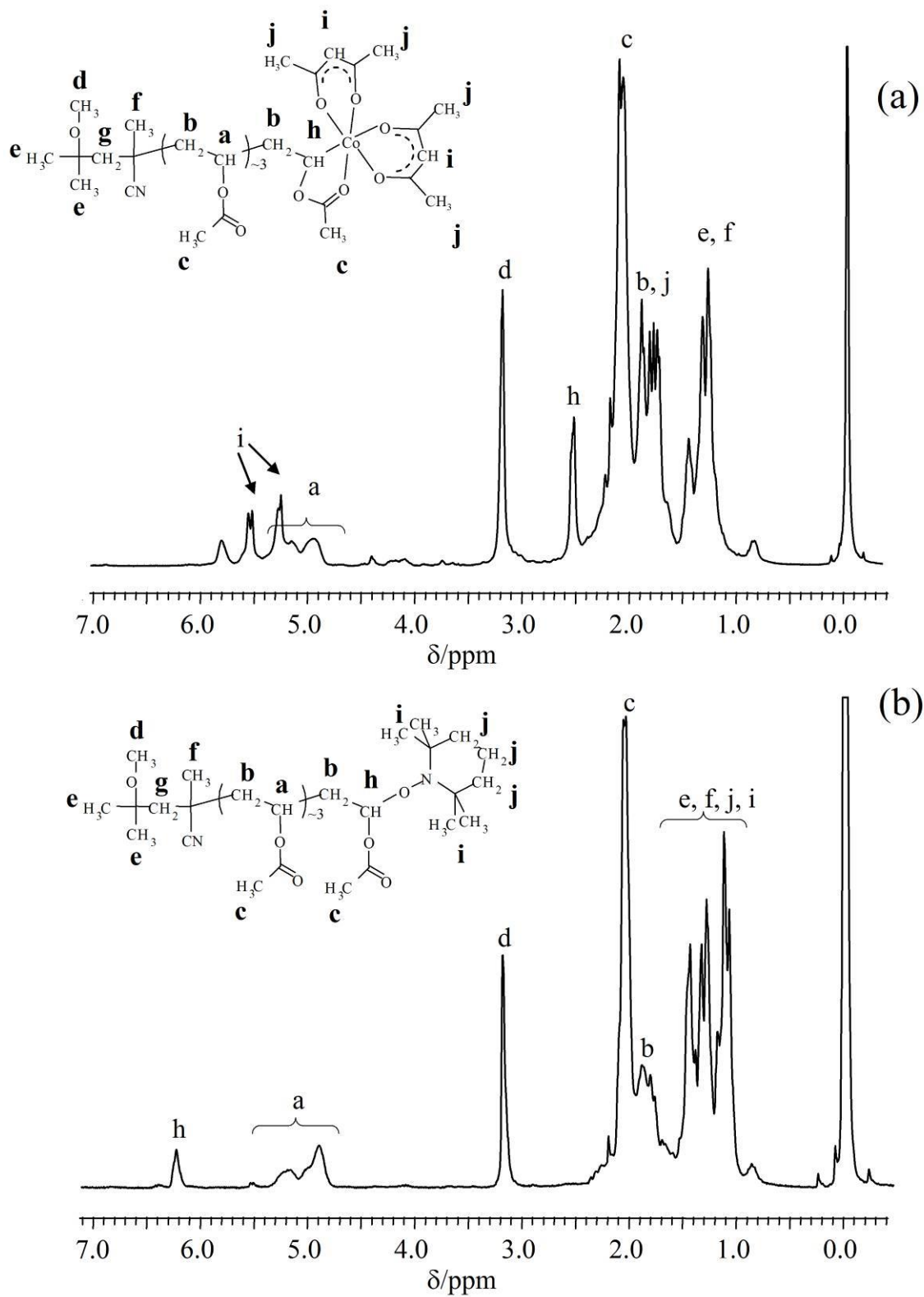


Figure 3. ^1H NMR spectrum for the low molecular weight cobalt adduct (2): (a) untreated; (b) after treatment with TEMPO (2'). Solvent = CDCl_3 .

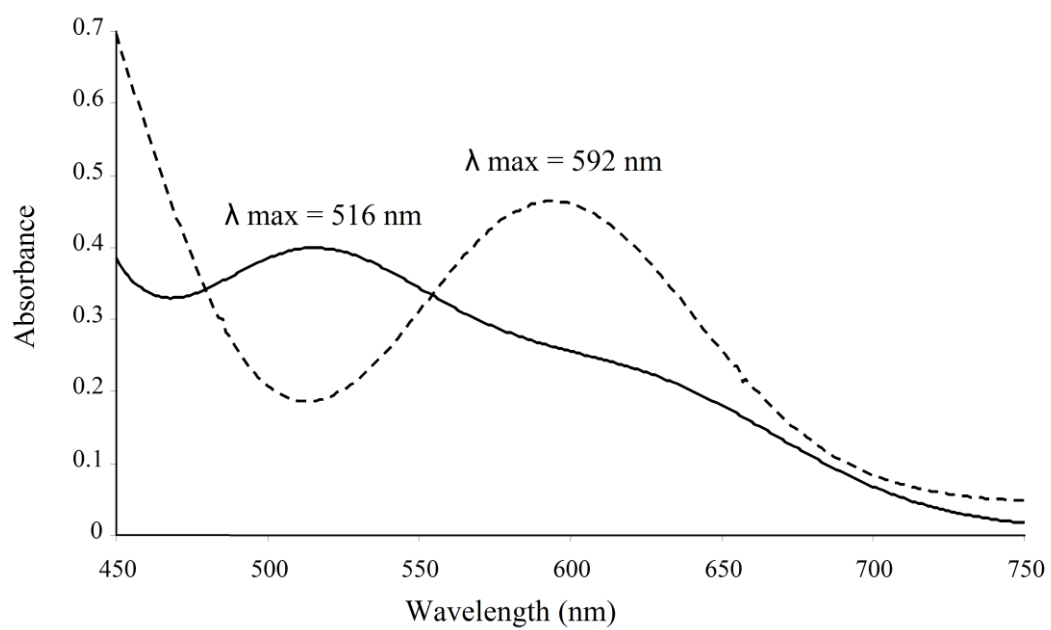


Figure 4. UV-visible spectra for the green compound **1** (dotted line, $\lambda_{\text{max}} = 592$ nm) and the pink compound **2** (full line, $\lambda_{\text{max}} = 516$ nm and 613 nm) in degassed CH_2Cl_2 .

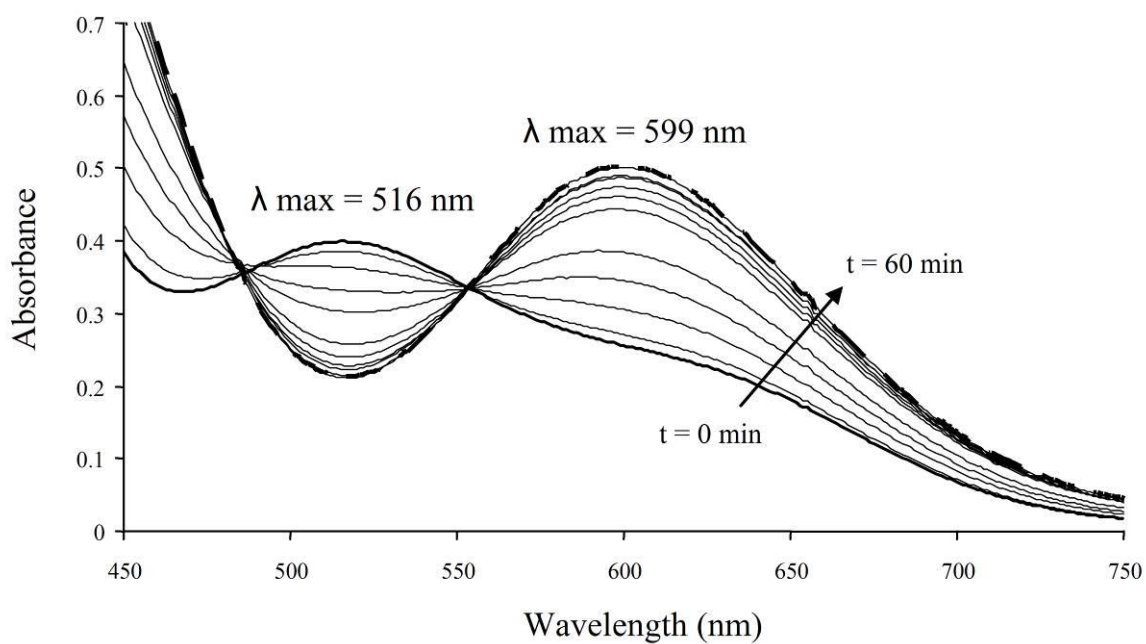


Figure 5. Evolution of the UV-visible spectrum of the pink compound **2** (broad full line, $\lambda_{\max} = 516$ nm) in degassed CH₂Cl₂ when exposed to air. Spectra were collected every 5 minutes for 60 minutes until the color turned green (compound **3**, broad dotted line, $\lambda_{\max} = 599$ nm).

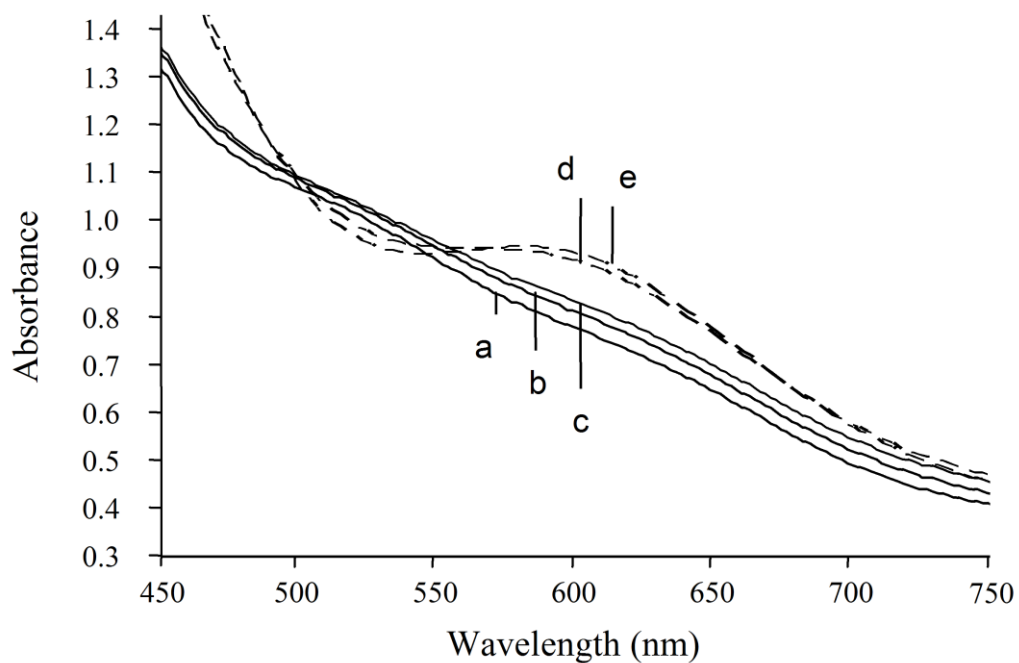


Figure 6. Evolution of the UV-visible spectrum of the pink cobalt adduct **2** in a degassed acetone/water mixture (9.5/0.5) (full lines) (a) $t = 0$, (b) $t = 20$ min, (c) $t = 40$ min under inert atmosphere, before exposure to air for 4 min between each scan (dotted lines) at (d) $t = 60$ min, (e) $t = 100$ min.

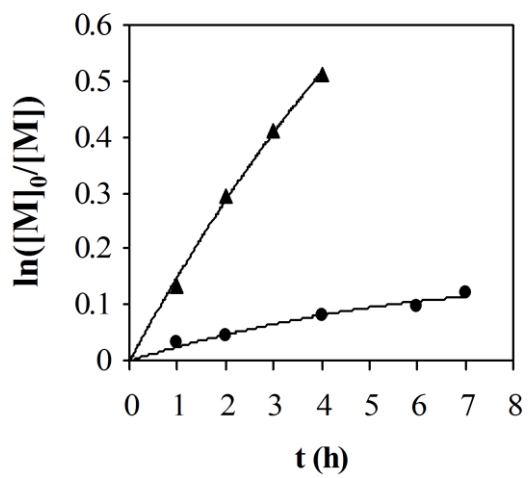


Figure 7. Time dependence of $\ln([M]_0/[M])$ for the VAc polymerization initiated by the green compound **1** (▲) and the pink compound **2** (●). (Table 1, entries 1 and 2, respectively)

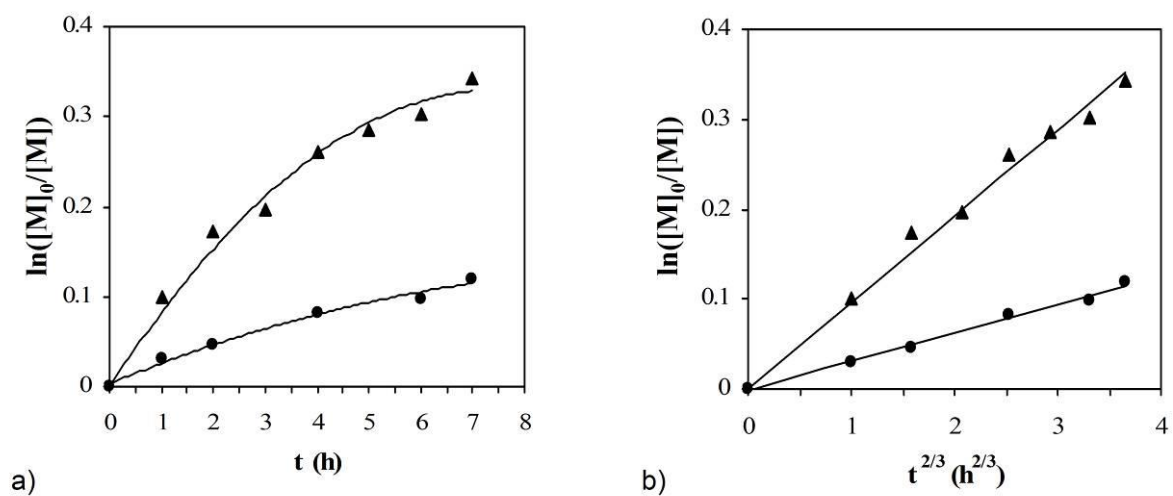


Figure 8. a) First and b) 2/3-order dependence of $\ln([M]_0/[M])$ on time for the VAc polymerization initiated by the pink compound **2** with (▲) and without (●) pyridine (Table 3 and entry 2 of Table 1, respectively).

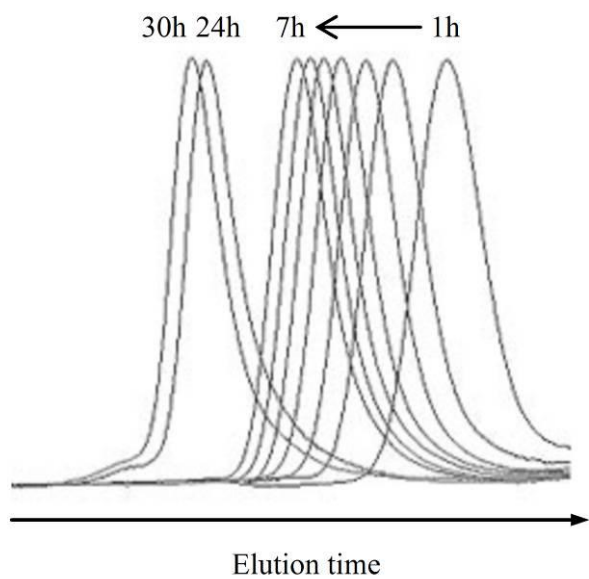


Figure 9. Evolution of SEC chromatograms with time for the VAc polymerization initiated at 30°C by the pink cobalt adduct **2** in the presence of a stoichiometric amount of pyridine (Table 3).

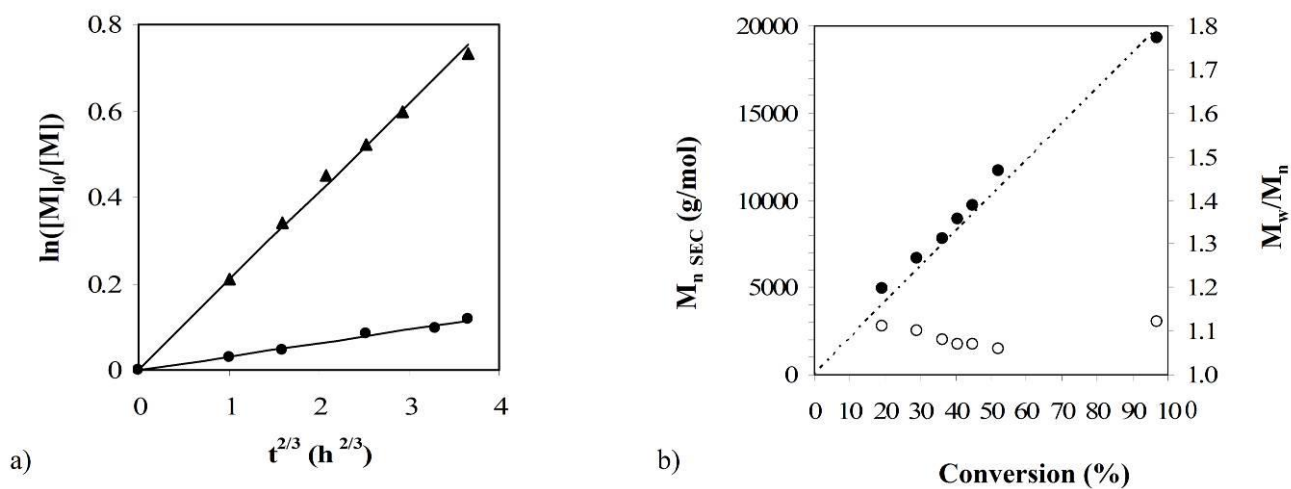


Figure 10. a) 2/3-order time dependence of $\ln([M]_0/[M])$ for the VAc polymerization initiated by the pink cobalt adduct **2** with (\blacktriangle) and without (\bullet) water (Table 4 and entry 2 in Table 1, respectively). b) Dependence of the molar mass (\bullet) and molar mass distribution (\circ) for the VAc polymerization initiated by the pink cobalt adduct **2** in the presence of water (Table 4). The dotted line is the theoretical prediction based on the $[VAc]/[Co]$ ratio.

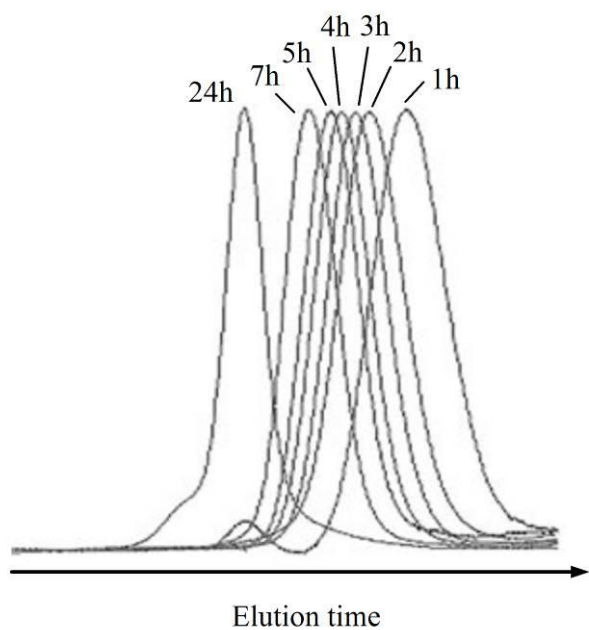


Figure 11. Evolution of the SEC chromatograms of PVAc with the polymerization time. This polymerization was initiated by the pink cobalt adduct **2** added with water at 30°C. (Table 4)

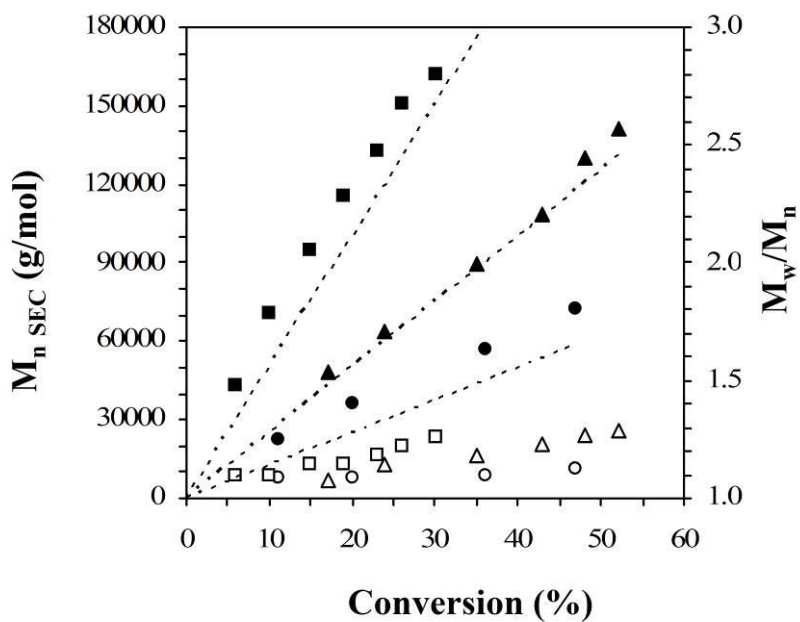


Figure 12. Dependence of the molar mass (full symbols) and molar mass distribution (hollow symbols) for the VAc polymerization initiated by the pink cobalt adduct **2** in the presence of water, at different [VAc]/[Co] ratios. The dotted lines correspond to the theoretical molar masses calculated from the [VAc]/[Co] ratios and VAc conversions. Conditions : 40°C, pink cobalt adduct **2** (0.0185 mmol), H₂O (2.22 mmol), VAc (●, 27.0 mmol) (▲, 54.0 mmol) (■, 108.0 mmol).

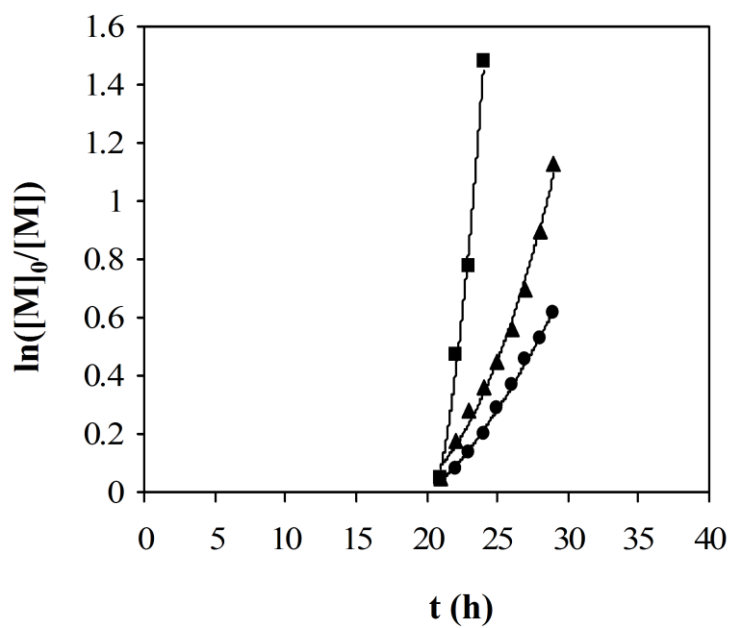


Figure 13. Plot of $\ln([M]_0/[M])$ versus time for the vinyl acetate polymerization in the presence of $\text{Co}(\text{acac})_2$ at 30°C .
 Conditions : 21h of pre-reaction $[\text{VAc}]/[\text{Co}(\text{acac})_2]/[\text{V-70}] = 540/1/3$ then (●) no water added (▲) water saturated VAc (■) biphasic system : $V_{\text{VAc}}/V_{\text{H}_2\text{O}} = 4$.

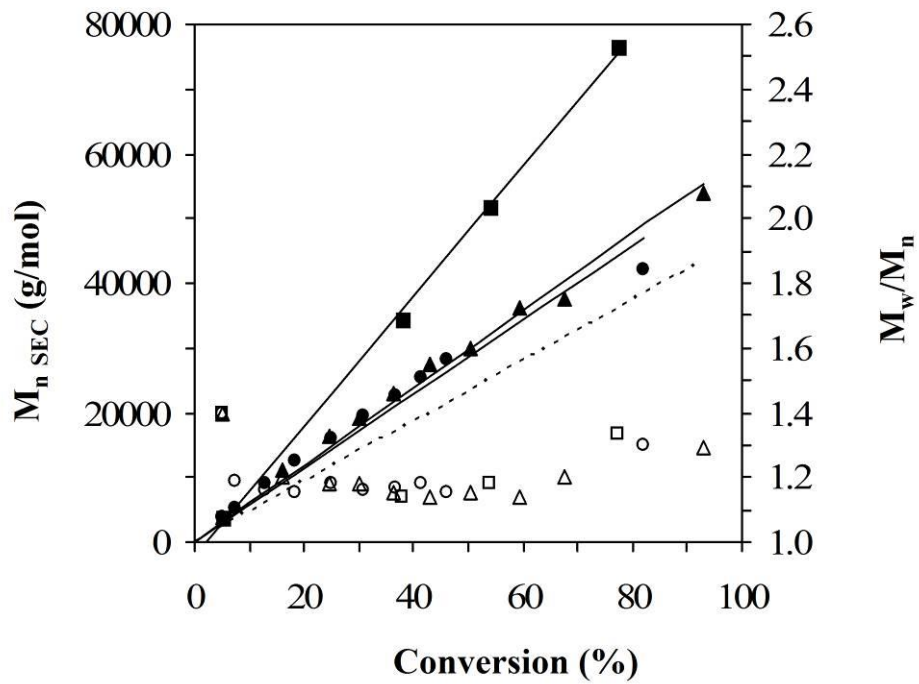


Figure 14. Dependence of the molar mass (full symbols) and molar mass distribution (hollow symbols) on the monomer conversion for the vinyl acetate polymerization in the presence of $\text{Co}(\text{acac})_2$ at 30°C . Conditions : 21h of pre-reaction $[\text{VAc}]/[\text{Co}(\text{acac})_2]/[\text{V-70}] = 540/1/3$ then (●,○) no water added ($f = 0.82$), (▲,△) water saturated VAc ($f = 0.78$), (■,□) two-phase system : $V_{\text{VAc}}/V_{\text{H}_2\text{O}} = 4$. ($f = 0.46$).

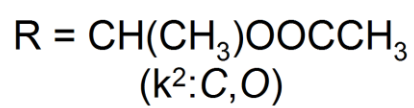
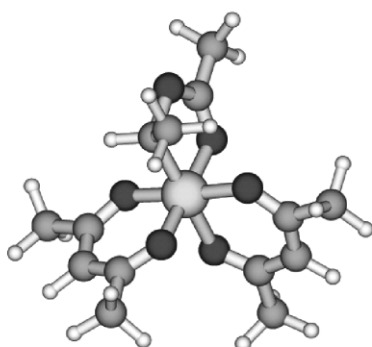
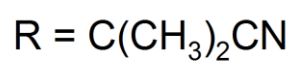
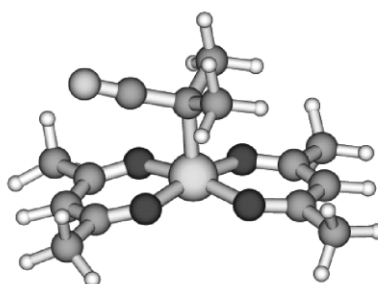
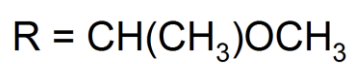
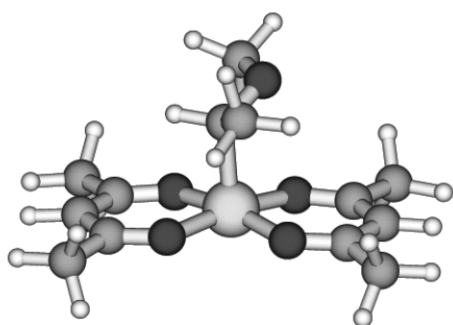
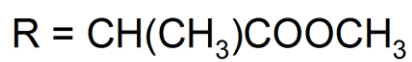
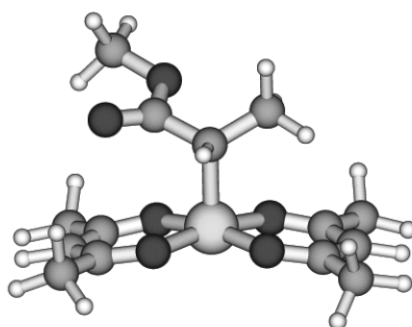
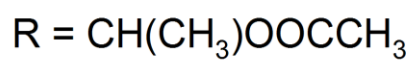
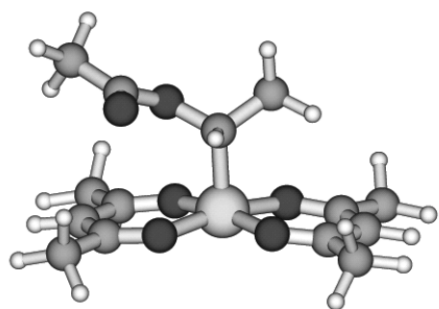


Figure 15. DFT optimized geometries of the model compounds R-Co(acac)₂.

Table 1. CMRP of vinyl acetate initiated by different cobalt adducts

Entry	t (h)	Conv'n %	$M_{n, SEC}^a$ (g/mol)	$M_{n, th}^b$ (g/mol)	M_w/M_n
1	1	12.5	32200	3980	2.25
	2	25.6	50400	8600	1.88
	3	33.7	54800	11300	1.84
	4	40.0	55600	13200	1.89
2	1	3.0	907	620	1.20
	2	4.4	1120	902	1.24
	4	7.9	2180	1620	1.07
	6	9.3	2860	1900	1.07
	7	11.3	3400	2320	1.07
3	24	/	/	/	/

Bulk polymerization in at 30°C. (1) Green compound **1** (0.140 mmol) / VAc (54.0 mmol). (2) Pink compound **2** (0.227 mmol) / VAc (54.0 mmol). (3) Green compound **3** (0.227 mmol; resulting from exposure of the pink compound **2** to air for 16h) / VAc (54.0 mmol). ^a $M_{n, SEC}$ in THF with a PS calibration. ^b Calculated from the [VAc]/[Co] ratio and conv. The cobalt concentration was determined by ICP.

Table 2. CMRP of VAc initiated by the pink cobalt adduct **2** in the presence of V-70 at 40°C.

	t (h)	Convsn (%)	M _n SEC ^a (g/mol)	M _n th ^b (g/mol)	M _w /M _n
1	1	3.7	/	/	/
	2	4.0	7800	10000	1.10
	3	6.6	16600	16600	1.05
	4	8.4	20100	21100	1.07
	5	9.9	23800	24900	1.08
2	1	8	16600	20100	1.11
	2	16	32300	40200	1.14
	3	33	63500	83000	1.25
	4	49	78000	123100	1.31
	5	55	94700	138200	1.43

At 40°C. Pink cobalt adduct **2** = 0.0185 mmol (determined by ICP). 1) VAc = 54.0 mmol. 2) 54.0 mmol, V-70 = 0.02 mmol (soit [Co]/[V-70] = 0.925). ^a M_n SEC in THF with a PS calibration. ^b Calculated from the [VAc]/[Co] ratio and conv. The cobalt concentration was determined by ICP.

Table 3. CMRP of VAc initiated by the pink cobalt adduct **2** in the presence of pyridine

time (h)	Conv'n (%)	$M_{n, SEC}^a$ (g/mol)	$M_{n, th}^b$ (g/mol)	M_w/M_n
1	9	3140	1950	1.06
3	18	5500	3700	1.06
5	25	7100	5100	1.07
7	29	8600	6000	1.07
24	54	15400	11100	1.09
30	61	17000	12300	1.10

Bulk polymerization at 30°C. Pink cobalt adduct **2** (0.227 mmol) / VAc (54.0 mmol)/ pyridine (18mg, 0.229 mmol). ^a $M_{n, SEC}$ in THF with a PS calibration. ^b Calculated from the [VAc]/[Co] ratio and conversion. The cobalt concentration was determined by ICP.

Table 4. CMRP of VAc initiated by the pink cobalt adduct **2** in the presence of water

t (h)	Conv _n (%)	M _n SEC ^a (g/mol)	M _n th ^b (g/mol)	M _w /M _n
1	19	4900	3900	1.11
2	29	6700	5900	1.10
3	36	7800	7400	1.08
4	41	8900	8300	1.07
5	45	9700	9200	1.07
7	52	11700	10600	1.06
24	97	19300	19800	1.12

Bulk polymerization at 30°C. Pink compound **2** (0.227 mmol) / VAc (54.0 mmol)/ H₂O (2.22 mmol) ^a M_n SEC in THF with a PS calibration. ^b Calculated from the [VAc]/[Co] ratio and monomer conversion. The cobalt concentration was determined by ICP.

Table 5. Co-R bond dissociation enthalpies and relevant optimized geometrical parameters for the R-Co(acac)₂ molecules.

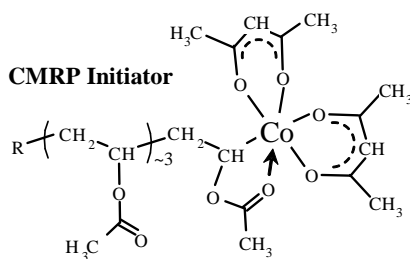
R	Co-R BDE (kcal/mol)	Co-R distance (Å)
CH ₃ ^a	14.55	1.921
CH(CH ₃)OCH ₃	8.45	1.987
CH(CH ₃)OOCCH ₃	5.73	1.957
CH(CH ₃)OOCCH ₃ (κ ² :C,O)	11.92	1.997
CH(CH ₃)COOCH ₃	-1.50	1.983
C(CH ₃) ₂ CN	-5.52	2.007

^a From ref. ³⁶

((Catch Phrase))

A. Debuigne,^a Y. Champouret,^b R.
Jérôme,^a R. Poli^{*b}, C.
Detrembleur^{*a}

**Mechanistic Insights into Cobalt
Mediated Radical Polymerization
(CMRP) of Vinyl Acetate via
Cobalt(III) Adducts as Initiators**



The key factors governing the intimate mechanism of the cobalt mediated radical polymerization (CMRP) of vinyl acetate were studied using cobalt(III) adducts as initiating species. Mechanistic insights into CMRP were supported by kinetics data and DFT calculations.